MULTIVARIATE DYNAMIC CONTROL OF A GIS-BASED SPATIALLY-VARIABLE APPLICATOR

BY

MIN-WEN WANG

A DISSERTATION PRESENTED TO THE GRADUATE SCHOOL
OF THE UNIVERSITY OF FLORIDA IN PARTIAL FULFILLMENT
OF THE REQUIREMENTS FOR THE DEGREE OF
DOCTOR OF PHILOSOPHY

UNIVERSITY OF FLORIDA

1994

ACKNOWLEDGEMENTS

The author would like to express his gratitude and appreciation to the members of his supervisory committee, Dr. John K. Schueller, Dr. Jiri Tlusty, Dr. Jacob Hammer, Dr. Sencer Yeralan, and Dr. Scot E. Smith, for their assistance and guidance.

The author is especially grateful to his advisor, Dr. John K. Schueller, for suggesting the research topic and for his encouragement and patience throughout the research.

The author would like to thank Mr. Karl Wild of the Technical University of Munich-Weihenstephan for supplying the field data used in this research.

The author would also like to express his deepest appreciation to his family and his beloved wife Chiu-Hsia for their spiritual encouragement and support.

TABLE OF CONTENTS

ACKNOWLEDGEMENTS ii

ABSTRACT vi

CHAPTERS

1 INTRODUCTION 1
Field Variability 1
Spatially-Variable Control 2
Spatial Data Management System 3
Positioning System 3
Fertilizer/Pesticide Applicator System 4
Efficiency of Existing System 6
Scope of the Study 6

2 SPATIALLY-VARIABLE DATA HANDLING SYSTEM 9
Geographic Information System 9
Geo/SQL GIS System 9
Spatial Data Base Design Considerations 10
Attribute Table 10
Polygon Object 11
Cell Size Selection 11
GIS Data Base Design Using Geo/SQL 12
Digitizing the Map 13
Defining GeoView 13
Preparing and Tagging the Field 14
Query 14
Determinate Fertilizer Desired Rate 16

3 ANALYSIS OF SPRAYING SYSTEM 21
Introduction 21
Experimental Setup 22
State-Space Models of the Spraying System 23
Single Pump System 24
Dual-Pump System 27
Numerical Values of Dual-Pump System Model 31
Summary 32

4 CONTROL OF FLUID SPRAYING SYSTEM 39
Introduction 39
Discretization of Continuous Model 40
System Controllability and Observability 41
Linear Quadratic Gaussian Problem 42
Steady-State Linear Quadratic Regulator 43

Kalman Filter 44
Sprayer System Analysis 45
Variation of Model Parameters 47
Closed-Loop Control System Design 48
LQR Design 49
Kalman Filter Design 51
Experimental Results 52
Effects of Measurement Covariance 52
Results with Different Configurations 54
Closed-Loop and Open-Loop Performance 54

5 SELECTION OF BOOM HOSE DIAMETER 76
Introduction 76
Flow Distribution in the Boom 77
Application Errors 80
Dynamic Response 81
Transportation Delay 82
Application Error Formulation 84
Separated-Mixture System Application Error 87
Optimal Diameter and Precommand Time 88
Test Cases 89
Mixture Changing Ratio 90
Cell Size Effect 90
System Dynamic Effect 91
Flow Rates Variation Effect 91
Summary 91

6 SIMULATION WITH FIELD DATA 104
Introduction 104
Pump Flow Rate 104
Simulations of Small Scale Spraying Systems 106
Combined-Mixture System 106
Separated-Mixture Systems 107
Simulation Results 107
Simulations of Large Scale Spraying Systems 108
Combined-Mixture System 108
Separated-Mixture Systems 108
Simulation Results 109
System Performance Comparison 109

7 CONCLUSIONS AND RECOMMENDATIONS 121
Conclusions 121
Recommendations 122
Design Recommendation 122
Future Research Recommendation 123

APPENDICES

A PROGRAM FERTILIZER.C 125

B PROGRAM DP.C 127

C PROGRAM POWELL.C 133
REFERENCES 146
BIOGRAPHICAL SKETCH 151

Abstract of Dissertation Presented to the Graduate School of the University of Florida in Partial Fulfillment of the Requirements for the Degree of Doctor of Philosophy

MULTIVARIATE DYNAMIC CONTROL OF A GIS-BASED SPATIALLY-VARIABLE APPLICATOR

By

Min-Wen Wang

August 1994

Chairman: Dr. John K. Schueller
Major Department: Mechanical Engineering

Spatially-variable control of fertilizer and pesticide application has a great potential to increase benefit from crop yield and significantly reduce the introduction of fertilizers and pesticides into the environment. However, inaccuracies in application rate control and application errors caused by system dynamics, nonuniform distribution of flow characteristics, and mixture transportation delay will reduce that potential.

In this research, state-space models of selected liquid spraying systems were derived. Optimal pump flow rate control using Linear Quadratic Gaussian (LQG) control theory was conducted on a dual-pump spraying system. Pump flow rate estimation using a pressure transducer has be implemented with a Kalman filter.

A Geo/SQL GIS based field data handling system was built to automatically determine application rates for spatially-variable controlled liquid fertilization. Field data from a German field was used to build the spatial database.

Tools for analysis and design of spraying systems were developed. The flow characteristics along a boom hose has been studied as a divided flow manifold problem. Application error caused by system transient response, nonuniform flow distribution, and transportation delay was formulated. Optimal boom hose diameter and precommand time concepts based on minimizing integral absolute application error were derived and examples were demonstrated. Programs for flow characteristic and optimal boom hose diameter and precommand time selection were developed.

Overall this study supports the development of engineering techniques for designing spatially-variable liquid fertilizer/pesticide application.

CHAPTER 1
INTRODUCTION

Field Variability

Fields used to produce agricultural crops are not uniform by their nature. There are variations in soil properties, water and nutrient supplies, and infestation of pests for different spatial locations or positions in a field (Schueller, 1988). Buchholz and Wollenhaupt (1989) indicated that substantial phosphorus and potassium variability is common and found phosphorus varied from 16 to 150 lb/A when 80 acres were sampled for a 4 acre basis. Mulla and Hammond (1988) show that P and K variability can be even higher in a field. Paul's (1988) study shows that the pH values of a Wisconsin field varied from 5.5-7.1%. Anon. (1989) shows that the soil organic matter of an Indiana field ranges from 1.35% to 3.5%. Wilson and Scott (1982) observed a field for 6 years and found that blackgrass and wild oats were found in less than 40% of the field they observed. Miller et al. (1992) found that the grain yield can vary by more than 50% across the different landscape position. Kepple (1988) reported the cotton yield ranged over 900-1900 lb/A in a field.

Typical agricultural operators apply their fertilizer or pesticide at a constant rate equal to that required by the area of greatest need in a given production unit (Schueller,

1992). This results in an overapplication in most of the field. About 4 billion pounds of pesticide are used annually in the United States (Schueller, 1992) and the U.S. fertilizer annual consumption rate is greater than 19 million metric tons (FAO, 1983). To improve the economic efficiency and environmental protection, there have been attempts to manage fields according to the variabilities of the fields. This is known as spatially-variable fertilizer/pesticide control.

Spatially-Variable Control

Schueller (1992) indicated DICKEY-john, the American agricultural electronics firm, was reportedly involved in spatially-variable research and development in the late 1970s, but it is difficult to determine the origins of public discussion of the concept. By the mid 1980s various forms of spatially-variable control were advocated (Anson, 1983; Hummel, 1985). Schueller (1988) had shown the overall spatially-variable fluid fertilizer applicator design concept.

The key elements of a spatially-variable fertilizer/pesticide application system are a spatially-variable data management system, a positioning system, and a fertilizer/pesticide applicator system. The data management system will store the spatial variables and required rates of fertilizers in a map. The positioning system will determine the position of the applicator system on the map and will allow the applicator to apply the proper fertilizer/pesticide rate on-the-go according to the fertilizer/pesticide rate map.

Figure 1.1 shows the diagram of a spatially-variable fertilizer application system.

Spatial Data Management System

In 1985, Ksiazek recognized the potential of spatially-variable control but felt that the applied technology was lacking to practically build a field database, determine applicator position, and compute the correct application rate for spatially-variable control. But recent work has advanced the technologies. Consider the field database. Geographic Information Systems (GIS) which have the ability to handle both spatial data and aspatial data (attribute) are now recognized by researchers (Schueller, 1992; Peterson et al., 1992) as a viable tool for spatially-variable control data management system. Although systems (Han et al., 1992; Motz, et al., 1993) have been developed and tested specially for spatially-variable control, commercial available GISs such as ARC/Info, GRASS, and Geo/SQL are still used by most of the researchers in this field. Data input to the data management system can include soil fertility data, soil nutrient contents, yield data, and pest infestation data. These data can be obtained through remote sensing, manual sampling and testing, or field operation of instrumented agricultural machinery. The data can be manipulated and an output of desired application rate maps can be generated.

Positioning System

A positioning system is needed to determine where the applicator is in a field. Soil Teq (1987) has developed SOILECTION to apply dry fertilizer using a Dead Reckoning system as a navigation system. Dead reckoning is a proven position determination technology but its accumulating error is a substantial difficulty. Triangulation from known locations is another positioning solution. Microwave triangulation was used by Bae et al. (1987) for spatially-variable mapping. The laser and radiowave triangulation methods have a disadvantage in that they are line of sight and they require fixed beacons or repeaters (Schueller, 1992). Most researchers consider the Global Positioning System (GPS) to be the best long-term locator alternative. GPS was developed by the U.S. Department of Defense. Each GPS satellite broadcasts a P code for military use and an C/A code for civilian use. Depending upon conditions of operation, the C/A code has an accuracy within 50 m. Positioning accuracy is improved with differential GPS (DGPS) which uses a known location fixed GPS reference station to determine a correction for the signal error of the mobile vehicle receiver. An accuracy within 6 m is achievable (Goering, 1992) on agricultural equipment using C/A code with a DGPS. Bobbe (1992) indicates that DGPS techniques were used to achieve 2-5 meter position accuracy. Tests by agricultural engineers in the U.K. (Stafford and Miller, 1992) and Montana

State University (Petersen, 1991) have even shown that a resolution of 2 m is possible using DGPS. Rapid technology and equipment development are rapidly decreasing the costs and inaccuracies of GPS receivers.

Fertilizer/Pesticide Applicator System

In spatially-variable control, the applicator should have the ability to change the fertilizers/pesticides application rates on-the-go. Centrifugal pumps and diaphragm pumps are the most common pumps used in spraying systems for fertilizer/pesticide application. Traditional spraying systems were designed to apply a single chemical mixture with a constant concentration rate and flow rate. Control was done through recirculating flow with a relief valve or controlling the speed of the pump. Two types of spraying systems based on the traditional spraying systems could be used for spatially-variable control application. The first type is a separated-mixture spraying system which is equipped with a multi-subsystem in an applicator and each subsystem sprays a mixture through its own boom and nozzles. The second type is combined-mixture spraying system in which the mixture components are combined and mixed before entering the boom hose and sprayed out through the boom hose's nozzles.

Separated-mixture design is currently used in SOILECTION's spatially-variable liquid fertilizer applicator system due to customer familiarity. The complicated and redundant structure of the boom hoses and nozzles is its major

drawback. Patel (1990) has studied a combined-mixture system using two commercially available electric motor-driven pump spraying systems, and study results indicate that different mixture can be fully mixed before the mixtures reach the nozzles. Wang (1991) has studied the dynamics of the spraying systems and results have shown that this combined-mixture type of system can be used for spatially-variable application.

Efficiency of Existing System

SOILECTION systems for spatially-variable control of dry and liquid application are commercially available. These systems use a microprocessor to control the applicator and store the desired application rate map in a PROM (Programmable Read Only Memory) chip (Elliott, 1987). Each chip allows only one specified application and the information in a chip is not changeable. As spatial data change, a new chip has to be programmed.

The existing spatially-variable liquid fertilizer control system uses a lookup table for flow rate control without considering the dynamic effects of the spraying system. This can be improved by a closed-loop feedback controller. In addition, the systems have been designed in a traditional manner, without detailed consideration of the characteristics of spatially-variable control.

Scope of the Study

The major objective of this project is to combine the techniques of control and a geographic information system into

an integrated method of analysis which considers both the spatial and the time-dynamic aspects of spatially-variable control in liquid fertilizer/pesticide applicator application. The major objective was accomplished in three aspects: building a GIS spatially-variable data management system, achieving optimal control of pump flow rates of spraying systems, and developing tools for analysis and optimal design of spraying systems.

In Chapter 2, a spatially-variable data management system for fertilizer application will be developed based on the Geo/SQL GIS. Design considerations and the process will be discussed with field data obtained from a German field. This system will determine proper fertilizer application rates based upon collected data. In Chapter 3, a state-space representation of a spraying system will be derived and will be used for optimal control in Chapter 4. Using LQG control theory for a dual-pump system, a flow rate control system will be derived and implemented in Chapter 4. Chapter 5 deals with flow characteristics in a boom hose and application error caused by transient response, nonuniform flow distribution, and mixture transportation delay. Optimal selection of boom hose diameter and control precommand time concept will also be presented in Chapter 5. Simulation of an applicator traveling on the German field will be performed in Chapter 6 with different type of spraying systems. Finally, conclusions and recommendations for future work are given in Chapter 7.

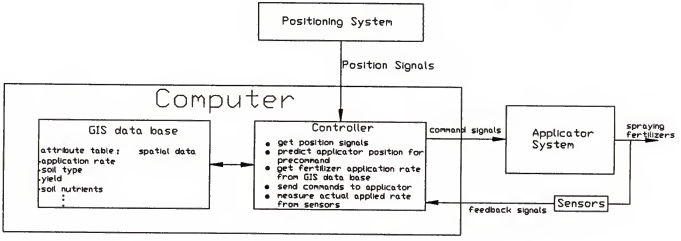

Figure 1.1 Spatially-Variable Fertilizer Application System Diagram.

CHAPTER 2
SPATIALLY-VARIABLE DATA HANDLING SYSTEM

Geographic Information System

A Geographic Information System (GIS) is an information system that works with data referenced by spatial coordinates. It is a database with capabilities of handling both spatial and aspatial data. The use of GIS has grown dramatically in the 1980s from obscurity to become commonplace in business, universities and governments (ESRI, 1991). Applications in land use (Dale, 1991; Kruse, 1989; Whalley and Schoolmaster, 1989), navigation (White, 1991), nature resource (Johnston, 1989; Shih, 1989), urban planning (Taylor and McDonald, 1989), and soil information (Burrough, 1991) have been reported. In this chapter, spatially-variable data handling using GIS in fertilizer application will be discussed. Field data obtained from Mr. Karl Wild of the Technical University of Munich-Weihenstephan will be used to build up the database.

Geo/SQL GIS System

Based upon their methods of storing data, GISs can be cataloged into raster-based GIS and vector-based GIS. A Geo/SQL vector-based GIS was received as a grant from Generation 5 Technology to provide the software needed for handling the spatially-variable data. Geo/SQL stands for geographic structural query language. It is a database

software which manages not only text and numbers but also geographic or spatial objects. It uses AutoCAD as a graphic tool for displaying, digitizing and editing maps and attributes of elements in the front-end. In the back-end Geo/SQL uses an Oracle SQL database management system to store and retrieve attribute data from Oracle databases. The Geo/SQL geography information system, integrated with AutoCAD and Oracle SQLPLUS, was used to handle the spatially-variable data of this research. To integrate the three software packages together, an IBI 386 personal computer with an additional 8 MB of RAM memory was used to enable these three softwares to run at same time. A Calcomp 12" by 12" digitizer table was added to the computer for digitizing maps.

Spatial Database Design Considerations

A spatial database usually includes spatial object and attribute data. The major spatial object types are point, line, polyline, or polygon. Attribute data are usually used to represent quality or quantity of the object and could be either numerical or text data. In a GIS, the attribute data are typically stored in a tabular formatted attribute table.

Attribute Table

The database to be designed is to determine P_2O_5 and K_2O fertilizer application rates. The application rates are determined by the spatial variables. In this prototype application, the variables were soil types, yield, predicted yield, and soil nutrient contents. The attribute table will

be designed to have columns of yield, soil type, soil P_2O_5 nutrient content, soil K_2O nutrient content, predicted yield, fertilizer P_2O_5 application rate, and fertilizer K_2O application rate. Another column needed is the zone# column which stores each zone's ID number for identifying.

Polygon Object

In spatially-variable control of fertilizer application, the field will be divided into zones (cells) and all the data within a zone will be averaged together. Spatial objects usually are treated as points, lines, polylines, or polygons in GISs. Each zone of the field will then be treated as a polygon object in the GIS database.

Cell Size Selection

The choice of cell size is one of the most important steps in spatially-variable control of fertilizer. A cell is a unit of spatially variable application. In a cell the spatial properties are considered to be uniform. Optimum cell size depends on many factors. The most important ones are spatial dependence of variables in the field and dynamic response of the applicator and the accuracy of the positioning system.

Soil sample semi-variograms have been used by soil scientists to determine the spatial variations of soil properties. Han et al. (1992) has proposed a mean correction distance (MCD) derived from the correlation of soil properties as a criterion to determine the upper limit of the cell size.

The defined MCD is the soil properties correlation distance. Two locations apart farther than MCD will have less correlation in soil properties. They then suggested that the upper limit of the cell size to be the minimum MCD of all spatial variables. In the study of Han et al. (1992), the MCD of soil nitrogen content (N) is 19.8 m and soil moisture is 54.8 m.

Schueller and Wang (1992) has shown that the fertilizer applicator dynamics will affect the efficiency of the spatially-variable control application. Positioning system accuracy also plays a big factor in selecting a proper cell size. To have the same percentage of pointing to the right cell, the more accurate the system the smaller the cell can be. Goering (1992) pointed out that to get a 85% confidence that the applicator is in the right cell the cell size should be at least twice the size of the positioning system accuracy. For example, if the GPS has an accuracy of 20 m, then the cell size should be at least 40 m to get 85% confidence that the applicator is inside the right cell.

GIS Data Base Design Using Geo/SQL

In a spatially variable application, a field is divided into the proper size of cells. All the properties of the field will be specified using the same cells, it then requires only one coverage (or layer) to store the spatial data. Although only one coverage is built to store the spatial data, the individual properties of the cells can be retrieved and

displayed in different property maps through query. Field data obtained from the Institut fuer Pflanzenbau and the Institut fuer Landtechnik of the Technical University of Munich-Weihenstephan were used in building the database of this study. The 3.74 hectare (9.24 acre) field was in southern Germany. Data which included wheat grain yield, soil type, soil test P_2O_5, and soil test K_2O were available. The yield data had been obtained with a grain combine instrumented with a grain flow sensor and a global positioning system (GPS) unit. Soil data were determined from manual soil tests. These data were input to the GIS database through the following procedure:

Digitizing the Map

The first step of building the database is digitizing the map. A plotted field map was digitized into a AutoCAD DWG drawing file in AutoCAD environment using the Summergraph digitizer. The completed map is shown in Figure 2.1 with cell size of 40 m.

Defining GeoView

A GeoView is a view that integrates spatial and attribute data information. When a query is executed GeoView will tell Geo/SQL where to get spatial or attribute data. A GeoView "GERMAN" was built in this database, it includes a Geo/SQL spatial data file called "G_FARM" and an Oracle attribute table called "ZONE". The table "ZONE" is defined with 9 columns which are Object #, yield, soil type, soil nutrient

P_2O_5, K_2O, predicted yield, FP_2O_5, and FK_2O (FP_2O_5 and FK_2O are the desired application rates for fertilizer P_2O_5 and K_2O).

Preparing and Tagging the Field

The next step is to prepare the drawing for data entry to spatial data files and the Oracle attribute table. Drawing errors such as incomplete polygons, gaps, and overlaps must be found and corrected. A TAG is then built in AutoCAD as a way of entering data into an attribute table corresponding to a particular geometric entity. The TAG can get data from keyboard entry, screen picks, or an automatic process. For this studied case a TAG was built where placement and activation of the cursor within a polygon prompted for keyboard entry of the required data. Data except fertilizer desired rates were tagged in TAG process. Oracle has the ability to interact with Microsoft C programs. After all the other data were tagged the fertilizer desired rates were updated according to the nutrient levels and soil types of the cells and are discussed in the next section.

The spatial geometric data were then INSERTed into Geo/SQL database files "G_FARM" and the tagged data INSERTed into an Oracle attribute table "ZONE". The resulting attribute table is shown in Table 2.1. In the soil type column, l is loam, t is clay, u is silt, and s is sand.

Query

Different properties of each cell of the field can be retrieved and classified through Geo/SQL query. By selecting

the proper menu driven query in Geo/SQL, a query can be formed automatically by Geo/SQL. After the query is executed, the results can be a drawing, a table or a file as defined by user. For example, from the Geo/SQL menu we can do

Select: POLYgons

From: ZONE

Select columns: SOIL_TYPE

Format: Objects

Options: Solid Fill

Options: Color

Set By: Lookup Table

Select Column: SOIL_TYPE

Lookup Table Name: SOIL.LUT

As: current drawing

Files: Execute

A Geo/SQL query will be formed and the query result will show on the screen as an AutoCAD drawing where different soil type of cell is solid filled with color according to the lookup table. The soil.lut lookup table lists what color the cell should be drawn according to soil type of the cell. Figure 2.1 is made through the above process except different hatch intensity was used to distinguish soil type instead of color solid fill of the cell. A similar query can be made to retrieve the other field data. Figures 2.2 to 2.7 show the maps for different field data.

Determinate Fertilizer Desired Rate

The fertilizer required rate was determined based on the "Die Duengung von Acker und Gruenland nach Ergebnissen der Bodenuntersuchung" (or roughly "The Fertilizing of Crop Fields and Pasture According to the Results of Soil Survey"). It depends on the predicted yield and the soil type. Mr. Karl Wild of the Technical University-Munich had done the predicted yield work for each zone using a somewhat crude model based upon soil type, past yield and climates. The soil P_2O_5 and K_2O nutrient levels are classified into categories A, B, C, D, and E. That order represents increasing fertility. The classification is shown in Table 2.2. The nutrient replacement needed for each zone was calculated for each zone based upon the assumption that each 10 dt (36.7 bu) of wheat removes 8 kgs (17.6 lbs) of P_2O_5 and 5 kgs (11 lbs) of K_2O. Table 2.3 specifies the desired application rate in kg/ha based upon the replacement "R" and the soil nutrient classification (A to E). Note that the K_2O classification depends on soil type. A program "FERTILIZER.C" was written according to Tables 2.2 and 2.3 to determine the fertilizers required rates and used to update the data into ORACLE "ZONE" table. This program is listed in Appendix A.

Table 2.1 Attribute Data of the Field

		SOIL			PRED. YIELD	FERTILIZER	
OBJECT#	YIELD	TYPE	P_2O_5	K_2O		P_2O_5	K_2O
1	5.9	Ltu	18	9	6.8	54.4	84
2	5.8	Ltu	21	27	6.6	52.8	33
3	5.7	Tu	26	8	7.2	28.8	136
4	5.8	Tu	8	12	6.1	88.8	80.5
5	6.8	Ltu	29	21	6.8	27.2	34
6	6.5	Ls3	37	34	6.4	25.6	16
7	7.3	Ls3	26	18	6.1	24.4	30.5
8	6.8	Ls3	28	23	6.4	25.6	32
9	6.9	Tu	32	32	6.9	27.6	34.5
10	7.2	Lu	28	22	7.5	30	37.5
11	7.4	Lu	27	34	7.7	30.8	19.25
12	7.5	Ls3	24	28	7.1	56.8	35.5
13	7.6	Lu	46	8	7.3	0	86.5
14	8.2	Lu	47	37	8.5	0	21.25
15	7.1	Lu	26	29	8.6	34.4	43
16	8.1	Lu	35	31	8.1	32.4	20.25
17	7.2	Lu	43	45	7.9	0	0
18	6.7	Lu	29	33	7.9	31.6	19.75
19	6.4	Ls3	29	37	7.1	28.4	17.75
20	6	Lu	61	33	7.5	0	18.75
21	6.1	Ls3	22	25	6.4	51.2	32
22	6.1	Ls3	27	25	6.8	27.2	34
23	5.5	Lu	18	21	7.3	58.4	36.5
24	6.4	Lu	28	31	7.7	30.8	19.25

Table 2.2 Soil Nutrient Classification

Classification	P_2O_5 (mg/100g)	K_2O (mg/100g)		
		light soil	medium soil	heavy soil
A - low	< 8	< 8	< 8	< 10
B - medium	8-14	8-14	8-14	10-19
C - high	15-25	15-20	15-30	20-35
D - very high	26-40	21-30	31-45	36-50
E - extremely high	> 40	> 30	> 45	> 50

Table 2.3 Desired Application (kg/ha)

Classification	P_2O_5	K_2O		
		light soil	medium soil	heavy soil
A - low	R+90	R+50	R+100	R+100
B - medium	R+40	R+25	R+50	R+50
C - high	R	R	R	R
D - very high	1/2 R	1/2 R	1/2 R	1/2 R
E - extremely high	0	0	0	0

R = Replacement for Crop Removal

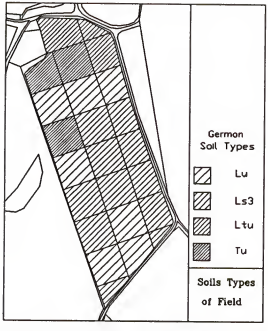

Figure 2.1 Soil Types of the Field.

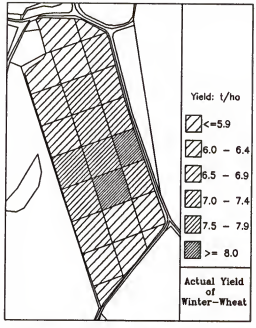

Figure 2.2 Wheat Grain Yield of the Field.

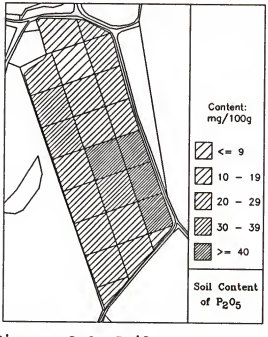

Figure 2.3 Soil Content of P_2O_5.

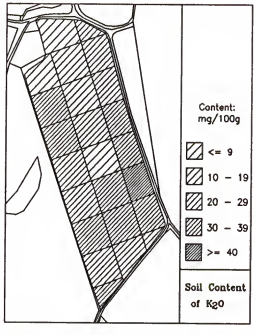

Figure 2.4 Soil Content of K_2O.

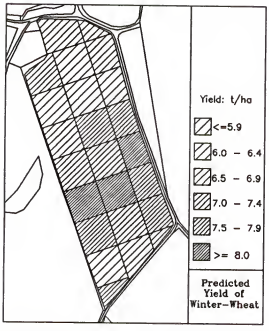

Figure 2.5 Predicted Yield of the Field.

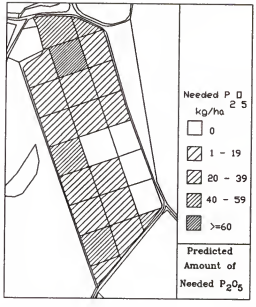

Figure 2.6 Desired Fertilization Rate of P_2O_5.

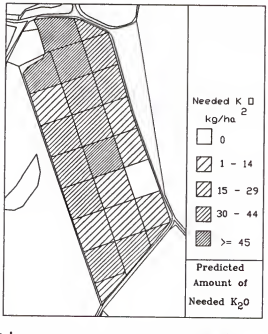

Figure 2.7 Desired Fertilization Rate of K_2O.

CHAPTER 3
ANALYSIS OF SPRAYING SYSTEM

Introduction

A fluid fertilizer/pesticide spraying system usually consists of a tank to contain mixtures, a means of driving the pump, a pump to pump the materials to be sprayed, and a boom system with nozzles to spray mixtures. The most common spraying systems are either belt driven, electric-motor driven, or hydraulic-motor driven pump systems. Commercially available fluid fertilizer/pesticide spraying systems usually contain only one tank and one pump to spray the mixture at a constant rate. The rate is often controlled by recirculation past a pressure relief valve. In spatially-variable control, the mixtures and rates of fertilizer components being applied have to be varied under accurate control. Therefore, systems with multi-tanks and multi-pumps are required.

Modelling of a single pump spraying system has been studied by Koo et al. (1987), Frost (1990), and Patel (1990) using experimental methods. Wang (1991) has derived a model for a spraying system based on the physical laws governing the system. The studied single pump spraying systems all had been classified as first order systems with a time delay. The spraying system model obtained by the previous researchers were all of experimental except Wang (1991) which used

mathematical equations to model the spraying systems. The experimental model could not be used when the system parameters are changed. In this project, a state variable representation of the electric motor driven dual pumps system model using the parameters obtained by Wang (1991) will be developed for designing the closed-loop control system.

In this chapter, experimental setup for this study will be discussed first and then the state-space system model will be developed.

Experimental Setup

Two commercial spraying systems, a Richie Best-Way Mini-Skid sprayer and a Bush Hog model MS 10 Mounted sprayer, were used in this study. Figure 3.1 shows a pictorial sketch of the experimental sprayer system with a boom and nozzles. The list of equipment is shown in Table 3.1. The spraying system was teed into a 1.93 m (76") long boom with five nozzles spaced 48 cm (19") apart. The boom hose's inner diameter was 1.27 cm (1/2"). On the Mini-Skid sprayer a SHURFlo integrated motor-pump unit was used to pump mixture from the 60 gallons tank to the boom. The pump is of diaphragm type and has an open flow delivery of 1.6 gpm. The motor is an armature-controlled DC motor rated at 12 V DC with a maximum 6 A applicable current. The Bush Hog sprayer, made by Flo-Jet, consists of a 10 gallon tank and an integrated pump-motor unit. The pump is also of diaphragm type and has a rated delivery of 1.35 gpm at 20 psi. The DC armature-controlled

motor is rated at 12 V DC with a maximum 8 A applicable current.

A GP50 pressure transducer was mounted at the end of the boom to measure the boom pressure. It has a proportional factor of 20 psi/V. There are three power supplies used in this experimental setup. An EPSCO 0 to 30 V DC, 0 to 10 A power supply was used to power the GP50 pressure transducer and it was called power supply 1 in Figure 3.1. Power supply 2 in Figure 3.1 is a Cole-Parmer Series 2630 power supply. This Cole-Parmer power supply can respond proportionally to inputs (1-20 ma, 0-5 V) from control instruments to 0-12 V DC (7 A maximum). It was used to power Mini-Skid motor and its voltage gain was adjusted to 2. Power supply 3 in Figure 3.1 is an HP MPB-5 Series Model 6286A DC power supply. Its operation mode was set so that the output voltage, ranging from 0 to 20 V DC (12 A maximum), in a 1 to 1 ratio with the input voltage. This power supply was used to power Bush Hog motor.

The digital side of the equipment consisted of a IBI 286 personal computer. A D/A and A/D accessory board, Data Translation model DT-2801 was installed in the computer for data acquisition and further system closed-loop control.

State-Space Models of the Spraying System

Figure 3.2 shows an single pump electric motor driven spraying system. In the spraying system, the motor drives the pump to deliver fluid to the boom; then the fluid flow into

the boom creates pressure in the boom that makes fluid come out of the nozzles in the form of a spray. The boom pressure also induces pump leakage and torque load on the motor.

Single Pump System

Wang (1991) has developed the spraying system model for single and dual pump systems with 5 nozzles. The model parameters he used are listed in Table 3.1 and these parameters will be used for this study. Using Wang's model and considering a system with N_z nozzles, a single pump spraying system model can be written as a combination of a motor characteristic equation and a flow continuity equation:

$$\tau_m \frac{dn}{dt} + n = K_{vn}(e_1 - K_{po}p) \tag{3.1}$$

$$\frac{V}{\beta}\frac{dp}{dt} = K_{nq}n - C_1 p - \frac{N_z C_d \sqrt{p}}{60} \tag{3.2}$$

where n = pump speed,

p = boom pressure,

e_1 = voltage input to motor,

and the others are system parameters listed in Table 3.1. This model is nonlinear and can be linearized at a operating point p_o, n_o, and e_{1o}. Defining $p=p_o+\delta p$, $n=n_o+\delta n$, and $e_1=e_{1o}+\delta e_1$, the continuity equation of the model can be then rewritten as follows

$$\frac{V}{\beta}\frac{dp}{dt}=K_{nq}n-C_1p-\frac{N_zC_d}{120\sqrt{p_o}}p-\frac{N_zC_d\sqrt{p_o}}{120} \tag{3.3}$$

Figure 3.3 shows the block diagram that represents the single pump model. A state-space representation of the model using p and n as state variables and e_1 as input can be derived as below

$$\frac{dx_1}{dt}=A_1x_1+B_1e_1+D_1 \tag{3.4}$$

where

$$x_1=\begin{pmatrix} n \\ p \end{pmatrix} \tag{3.5}$$

$$A_1=\begin{pmatrix} -\frac{1}{\tau_m} & \frac{-K_{vn}K_{pe}}{\tau_m} \\ \frac{\beta}{V}K_{nq} & -\frac{\beta}{V}\left(C_1+\frac{N_zC_d}{120\sqrt{p_o}}\right) \end{pmatrix} \tag{3.6}$$

$$B_1=\begin{pmatrix} \frac{K_{vn}}{\tau_m} \\ 0 \end{pmatrix} \tag{3.7}$$

$$D_1=\begin{pmatrix} 0 \\ -\frac{\beta}{V}\frac{N_zC_d\sqrt{p_o}}{120} \end{pmatrix} \tag{3.8}$$

This linearized model can also be represented using $\delta x_1=(\delta n,\delta p)^T$ as state variables and δe_1 as input as

$$\frac{d\delta x_1}{dt} = A_1 \delta x_1 + B_1 \delta e_1 \tag{3.9}$$

The variables that are of interest in this study are the flow rate of the pump and the pressure of the boom system. The relation of pump flow rate with motor speed n and pressure p is

$$q = K_{nq} n - C_1 p \tag{3.10}$$

Let q_o be the operating flow rate of pump and let $q = q_o + \delta q$, equation (3.10) can be rewritten as

$$x = \begin{pmatrix} q \\ p \end{pmatrix} = T_1 \begin{pmatrix} n \\ p \end{pmatrix} \tag{3.11}$$

or

$$\delta x = \begin{pmatrix} \delta q \\ \delta p \end{pmatrix} = T_1 \begin{pmatrix} \delta n \\ \delta p \end{pmatrix} \tag{3.12}$$

where

$$T_1 = \begin{pmatrix} K_{nq} & -C_1 \\ 0 & 1 \end{pmatrix} \tag{3.13}$$

Since $K_{nq} \neq 0$, the matrix T_1 is full rank. Through state transformation, the linerized model of the system with state variable x (or δx) can be represented as

$$\frac{dx}{dt} = T_1 A_1 T_1^{-1} x + T_1 B_1 e_1 + T_1 D_1$$
$$= Ax + Be_1 + D \tag{3.14}$$

or

$$\frac{d\delta x}{dt} = A\delta x + B\delta e_1 \tag{3.15}$$

where

$$A = \begin{pmatrix} -\frac{1}{\tau_m} - \frac{\beta}{V} C_1 & \frac{-C_1 - K_{nq} K_{vn} K_{pe}}{\tau_m} + \frac{\beta}{V} \frac{N_z C_d C_1}{120\sqrt{p_o}} \\ \frac{\beta}{V} & -\frac{\beta}{V} \frac{N_z C_d}{120\sqrt{p_o}} \end{pmatrix} \tag{3.16}$$

$$B = \begin{pmatrix} \frac{K_{nq} K_{vn}}{\tau_m} \\ 0 \end{pmatrix} \tag{3.17}$$

$$D = \begin{pmatrix} \frac{\beta}{V} \frac{N_z C_1 C_d \sqrt{p_o}}{120} \\ -\frac{\beta}{V} \frac{N_z C_d \sqrt{p_o}}{120} \end{pmatrix} \tag{3.18}$$

Dual-Pump System

A dual-pump spraying system consisting of the combination of a Mini-Skid sprayer and a Bush Hog sprayer is shown in Figure 3.1. For a dual-pump system, the model can be obtained by adding another motor characteristic equation into the single pump system and adding the second pump flow rate into the continuity equation of the single-pump system. The dual-pump model can be written as

$$\tau 1_m \frac{dn1}{dt} + n1 = K1_{vn}(e1 - K1_{pe}p) \tag{3.19}$$

$$\tau 2_m \frac{dn2}{dt} + n2 = K2_{vn}(e2 - K2_{pe}p) \tag{3.20}$$

$$\frac{V}{\beta}\frac{dp}{dt} = K1_{nq}n1 + K2_{nq}n2 - (C1_1 + C2_1)p - \frac{N_s C_d \sqrt{p}}{60} \tag{3.21}$$

Like the single-pump system, the dual-pump system model can be linearized at an operating point (p_o, $n1_o$, $n2_o$, $q1_o$, $q2_o$, $e1_o$, $e2_o$) with the definitions of $n2 = n2_o + \delta n2$, $q2 = q2_o + \delta q2$, and $e2 = e2_o + \delta e2$. The model represented in block form is shown in Figure 3.4 and the model represented in terms of state variable $z_1 = (n1, n2, p)^T$ and inputs $e = (e1, e2)^T$ is

$$\frac{dz_1}{dt} = A_{d1}z_1 + B_{d1}e + D_{d1} \tag{3.22}$$

where

$$A_{d1} = \begin{pmatrix} -\frac{1}{\tau_1} & 0 & \frac{-K1_{vn}K1_{pe}}{\tau_1} \\ 0 & -\frac{1}{\tau_2} & \frac{-K2_{vn}K2_{pe}}{\tau_2} \\ \frac{\beta}{V}K1_{nq} & \frac{\beta}{V}K2_{nq} & -\frac{\beta}{V}(C1_1 + C2_1 + \frac{N_s C_d}{120\sqrt{p_o}}) \end{pmatrix} \tag{3.23}$$

$$B_{d1}=\begin{pmatrix} \frac{K1_{vn}}{\tau_1} & 0 \\ 0 & \frac{K2_{vn}}{\tau_2} \end{pmatrix} \tag{3.24}$$

$$D_{d1}=\begin{pmatrix} 0 \\ 0 \\ -\frac{\beta}{V}\frac{N_z C_d \sqrt{P_o}}{120} \end{pmatrix} \tag{3.25}$$

Using state variables $\delta z_1=(\delta n1, \delta n2, \delta p)^T$ and inputs $\delta e=(\delta e1, \delta e2)$, the model is

$$\frac{d\delta z_1}{dt}=A_{d1}\delta z_1+B_{d1}\delta e \tag{3.26}$$

The state transformation matrix T_d between states z1=(n1,n2,p) and z=(q1,q2,p) is

$$T_d=\begin{pmatrix} K1_{nq} & 0 & -c1_1 \\ 0 & K2_{nq} & -C2_1 \\ 0 & 0 & 1 \end{pmatrix} \tag{3.27}$$

The linearized model of the dual-pump system can be represented as

$$\begin{aligned} \frac{dz}{dt} &= T_d A_{d1} T_d^{-1} z + T_d B_{d1} e + T_d D_{d1} \\ &= A_d z + B_d e + D_d \end{aligned} \tag{3.28}$$

or

$$\frac{d\delta z}{dt} = A_d \delta z + B_d \delta e \tag{3.29}$$

where

$$A_d = \begin{pmatrix} -\frac{1}{\tau_1} - \frac{\beta}{V} C1_1 & -\frac{\beta}{V} C1_1 & \frac{-C1_1 - K1_{nq} K1_{vn} K1_{pe}}{\tau_1} + \frac{\beta}{V} \frac{N_s C_d C1_1}{120\sqrt{P_o}} \\ -\frac{\beta}{V} C2_1 & -\frac{1}{\tau_2} - \frac{\beta}{V} C2_1 & \frac{-C2_1 - K2_{nq} K2_{vn} K2_{pe}}{\tau_2} + \frac{\beta}{V} \frac{N_s C_d C1_2}{120\sqrt{P_o}} \\ \frac{\beta}{V} & \frac{\beta}{V} & -\frac{\beta}{V} \frac{N_s C_d}{120\sqrt{P_o}} \end{pmatrix} \tag{3.30}$$

$$B_d = \begin{pmatrix} \frac{K1_{nq} K1_{vn}}{\tau_1} & 0 \\ 0 & \frac{K2_{nq} K2_{vn}}{\tau_2} \\ 0 & 0 \end{pmatrix} \tag{3.31}$$

$$D_d = \begin{pmatrix} \frac{\beta}{V} \frac{N_s C1_1 C_d \sqrt{P_o}}{120} \\ \frac{\beta}{V} \frac{N_s C2_1 C_d \sqrt{P_o}}{120} \\ -\frac{\beta}{V} \frac{N_s C_d \sqrt{P_o}}{120} \end{pmatrix} \tag{3.32}$$

One phenomenon can be found from equations 3.23 and 3.25 is that the linearized model of the dual-pump system varies according to the boom pressure changes. That also means that it varies according to total pump flowrates (q1+q2) and the ratio of q1 and q2 does not affect the system dynamics if the total flow rates are the same.

Numerical Values of Dual-Pump System Model

There are 3 kinds of nozzle tips used in this study and they are TeeJet Disc-Cone Type Spray Tips Orifice Disc Number D2, and D3 and TeeJet VisiFlo Flat Spray Tip XR11003VS (XR3). The nozzle tips' discharge coefficients were listed in Table 3.2. The parameters' numerical values listed in Table 3.1 were from Wang (1991) except that K_{vn}s, K_{pe}s, and C_ls which were obtained using least squares method from experimental data listed in Table 3.3.

Consider the dual-pump system with 5 D2 nozzle tips configuration, when the boom pressure is about 26 psi (both motor's were powered about 7 V DC), the model can be expressed as

$$\frac{dz}{dt}=\begin{pmatrix} -33.545 & -0.2117 & -5.602E\text{-}3 \\ -0.05146 & -25.05 & -3.735E\text{-}3 \\ 3649.6 & 3649.6 & -1.094 \end{pmatrix} z + \begin{pmatrix} 0.06 & 0 \\ 0 & 0.03765 \\ 0 & 0 \end{pmatrix} e + \begin{pmatrix} 1.64E\text{-}3 \\ 3.988E\text{-}4 \\ -28.285 \end{pmatrix}$$

The open-loop poles of the system in s domain are located at s=-2.34,-24.4, and -32.9 which shows that the system is stable with a dominant system time constant 0.43 seconds.

Matrix B_d of equation (3.28) and the first two columns of matrix A_d consist of only constant terms and eventually are not affected by operating pressure changes and total nozzle numbers. Table 3.4 listed the numerical model values and the system poles for the open-loop spraying system with different

configurations. This continuous time state-space models will be used in closed-loop control in next chapter.

Summary

In this chapter, continuous state-space models of single and dual-pump spraying systems have been developed. The state-space model of a multi-pump spraying system can be derived by combining all the motors' characteristic equations and combining all the pumps' flow rates in the continuity equation. From the linearized models developed, the system dynamics depends only on the total flow rate into the boom.

Table 3.1 Parameters of the Dual-Pump System

Parameter	Values, Description
$\tau 1_m$	0.03 sec, Mini motor-pump unit time constant
$\tau 2_m$	0.04 sec, Bush motor-pump time constant
V	0.274 gallon, Total system volume (pipe)
ß	1000 psi, System Eefective bulk modulus
$K1_{vn}$	3.02 rps/V, Mini Motor voltage-speed factor
$K2_{vn}$	4.3 rps/V, Bush Motor voltage-speed factor
$K1_{nq}$	5.96E-5 gps/rps, Mini pump speed-flow rate factor
$K2_{nq}$	3.5E-4 gps/rps, Bush pump speed-flow rate factor
$K1_{pe}$	0.0622 V/psi, Mini motor pressure-voltage factor
$K2_{pe}$	0.09 V/psi, Bush motor pressure-voltage factor
$C1_l$	5.8E-5 gps/psi, Mini pump leakage coefficient
$C2_l$	1.41E-5 gps/psi, Bush pump leakage coefficient

Table 3.2 Nozzle Discharge Coefficients

Nozzle Tip Type	Cd ($gpm/psi^{0.5}$)
D2	0.03658
D3	0.043
XR11003VS	0.0483

Table 3.3 Listing of Data used for Fitting K_{vn} and K_{pe}

A. Mini-Skid

Tip	D3		D2		XR3	
Vin	Pressure	Flowrate	Pressure	Flowrate	Pressure	Flowrate
4	3.379648	0.006588	9.581797	0.005662	3.277109	0.007286
5	4.750742	0.00781	13.43629	0.006704	4.743906	0.008767
9	6.698008	0.009274	17.86402	0.00773	6.586679	0.01033
9	8.92164	0.010703	23.24977	0.008819	8.650156	0.011838
9	11.71363	0.012264	29.80445	0.009985	11.62965	0.013726
9	13.41969	0.013127	34.84352	0.010796	13.07984	0.014557
10	15.51148	0.014113	38.73903	0.011384	14.89039	0.015532
9	4.414804	0.006023	6.684336	0.006305	4.426523	0.006775
5	6.5525	0.007338	9.586679	0.007551	6.488047	0.008767
9	9.087656	0.008642	12.90211	0.00876	8.902109	0.009607
9	11.90113	0.009889	17.0027	0.010056	11.76051	0.011043
9	15.68238	0.011352	22.20973	0.011493	15.53688	0.012692
5	18.53883	0.012343	25.94508	0.012422	17.91871	0.01363
10	20.97242	0.013127	28.83473	0.013095	20.10133	0.014437
9	6.85914	0.005631	4.880625	0.006734	6.48707	0.006151
5	10.02418	0.006807	7.095469	0.00812	9.493906	0.007441
6	13.40309	0.007871	9.717539	0.009503	12.81422	0.008645
7	17.51734	0.008999	12.73512	0.010878	16.77027	0.00989
8	22.79273	0.010264	16.90406	0.012533	21.84645	0.01128
9	26.49195	0.011066	19.51344	0.013466	25.67359	0.01223
10	29.3943	0.011657	21.9109	0.014269	28.44898	0.01288

B. Bush Hog

Tip	D3		D2		XR3	
Vin	Pressure	Flowrate	Pressure	Flowrate	Pressure	Flowrate
4	2.917734	0.006121	7.02125	0.004846	5.257578	0.005537
5	4.241953	0.00738	10.61402	0.005959	6.783945	0.00629
6	5.132578	0.008118	14.22926	0.006899	9.32789	0.007376
7	6.949961	0.009447	18.66773	0.007902	12.46949	0.008528
8	8.614023	0.010517	23.59352	0.008884	15.85816	0.009617
9	10.42457	0.01157	27.95777	0.009671	19.57008	0.010683
10	12.55641	0.012698	33.32692	0.010559	23.82691	0.011788
4	3.623789	0.005457	5.59839	0.00577	3.665781	0.006165
5	5.355234	0.006634	7.28101	0.00658	4.522226	0.006847
6	6.847422	0.007501	9.84449	0.007652	6.364023	0.008123
7	9.298594	0.008741	13.0232	0.008801	8.621836	0.009455
8	11.55348	0.009744	16.63453	0.009946	10.81031	0.010587
9	14.22047	0.01081	19.90016	0.010879	13.29371	0.01174
10	16.93336	0.011796	23.79176	0.011895	15.84352	0.012817
4	5.488047	0.005037	4.03882	0.006121	2.64625	0.006548
5	7.949961	0.006062	5.17164	0.006932	3.231211	0.007235
6	10.51832	0.006973	6.91675	0.008017	4.685312	0.008712
7	14.01637	0.008049	9.18921	0.009241	6.184336	0.01001
8	16.86305	0.008829	11.23902	0.010219	7.769297	0.011219
9	21.23219	0.009907	14.57203	0.011637	9.373789	0.012323
10	24.99879	0.01075	17.26637	0.012667	11.26246	0.013508

Table 3.4 Numerical Values of Continuous Models

Configuration	A_d	$(B_d:D_d)$	Poles
5 D3 Nozzle Tips at 20 psi	$\begin{pmatrix} -33.545 & -0.2117 & -5.5804E\text{-}3 \\ -0.05146 & -25.051 & -3.7294E\text{-}3 \\ 364.96 & 364.96 & -1.4644 \end{pmatrix}$	$\begin{pmatrix} 0.06 & 0 & 1.69E\text{-}3 \\ 0 & 0.03765 & 4.117E\text{-}4 \\ 0 & 0 & -29.2 \end{pmatrix}$	-2.73 -24.4 -32.9
3 D3 Nozzle Tips at 34.9 psi	$\begin{pmatrix} -33.545 & -0.2117 & -5.6268E\text{-}3 \\ -0.05146 & -25.051 & -3.1414E\text{-}3 \\ 364.96 & 364.96 & -0.66419 \end{pmatrix}$	$\begin{pmatrix} 0.06 & 0 & 1.344E\text{-}3 \\ 0 & 0.03765 & 3.268E\text{-}4 \\ 0 & 0 & -23.75 \end{pmatrix}$	-1.8 -24.54 -32.9
5 D2 Nozzle Tips at 25.6 psi	$\begin{pmatrix} -33.545 & -0.2117 & -5.602E\text{-}3 \\ -0.05146 & -25.051 & -3.7346E\text{-}3 \\ 364.96 & 364.96 & -1.094 \end{pmatrix}$	$\begin{pmatrix} 0.06 & 0 & 1.64E\text{-}3 \\ 0 & 0.03765 & 3.988E\text{-}4 \\ 0 & 0 & -28.285 \end{pmatrix}$	-2.34 -24.4 -32.9
3 D2 Nozzle Tips at 40 psi	$\begin{pmatrix} -33.545 & -0.2117 & -5.6347E\text{-}3 \\ -0.05146 & -25.051 & -3.1433E\text{-}3 \\ 364.96 & 364.96 & -0.5277 \end{pmatrix}$	$\begin{pmatrix} 0.06 & 0 & 1.224E\text{-}3 \\ 0 & 0.03765 & 2.976E\text{-}4 \\ 0 & 0 & -21.11 \end{pmatrix}$	-1.66 -24.5 -32.9
5 XR3 Nozzle Tips at 17.8 psi	$\begin{pmatrix} -33.545 & -0.2117 & -5.5644E\text{-}3 \\ -0.05146 & -25.051 & -3.7255E\text{-}3 \\ 364.96 & 364.96 & -1.739 \end{pmatrix}$	$\begin{pmatrix} 0.06 & 0 & 1.8E\text{-}3 \\ 0 & 0.03765 & 4.3741E\text{-}4 \\ 0 & 0 & -31.022 \end{pmatrix}$	-3 -24.4 -32.9
3 XR3 Nozzle Tips at 30 psi	$\begin{pmatrix} -33.545 & -0.2117 & -5.5644E\text{-}3 \\ -0.05146 & -25.051 & -3.7386E\text{-}3 \\ 364.96 & 364.96 & -0.8627 \end{pmatrix}$	$\begin{pmatrix} 0.06 & 0 & 1.4E\text{-}3 \\ 0 & 0.03765 & 3.396E\text{-}4 \\ 0 & 0 & -24.09 \end{pmatrix}$	-2 -24.4 -32.9

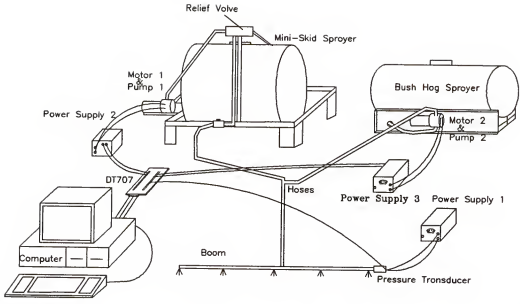

Figure 3.1 Schematic Diagram of the Experimental Dual-Pump Spraying System.

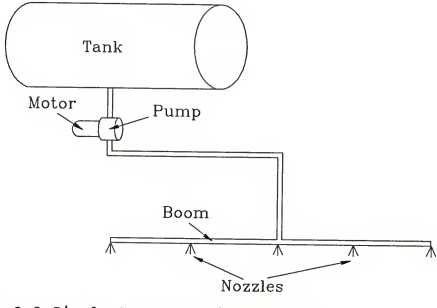

Figure 3.2 Single Pump Spraying System.

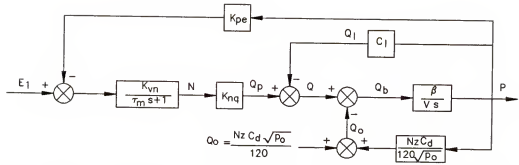

Figure 3.3 Block Diagram of a Single Pump Spraying System.

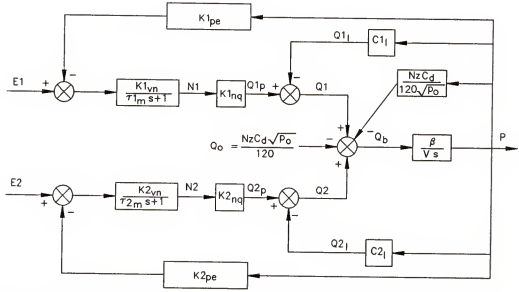

Figure 3.4 Block Diagram of a Dual-Pump Spraying System.

CHAPTER 4
CONTROL OF FLUID SPRAYING SYSTEM

Introduction

Most spatially-variable fertilizer application systems will have to apply multiple materials at varying rates simultaneously. They require multiple input, multiple output (MIMO) control systems. The existing systems use a lookup table for open loop flow rate control without considering the effects from dynamics of the spraying system. Through the study of spraying dynamic models, the key factors that dominate the system dynamics can be known and sophisticated closed-loop control algorithms can be applied to improve performance.

Practical physical systems subject to control are many times at best difficult to model deterministically and often only noisy observations of some of the state variables of system are available (Sage and White, 1977). Spraying systems are designed to work in a field environment where it is easy to suffer noises from the environment, other equipment, or disturbances. Linear Quadratic Gaussian (LQG) optimal control is a control theory that combines optimal control theory and optimal estimation techniques. It uses a Linear Quadratic Regulator (LQR) as a state feedback controller and a Kalman filter as an optimal state estimator. LQG is attractive

because it handles MIMO systems and because both LQR and Kalman filter are well known with excellent stability margins (Safonov and Athans, 1977).

For a control process with transient period which is short compared with process running time, optimal control and optimal estimation can be approached using a steady-state LQR and a steady-state Kalman filter. In the sprayer spraying process, the transient time is short compared with the period that a step command endures. Optimal control of spraying systems with a steady-state LQR and a steady-state Kalman filter will therefore be developed in this chapter.

Discretization of Continuous Model

To control a continuous system with a digital computer, the system model has to be discretized. A continuous linear system usually can be represented with the state differential equation

$$\frac{dx}{dt}=Fx+Gu \tag{4.1}$$

and the output equation

$$y=Hx \tag{4.2}$$

Assuming the control is applied from the computer with a zero order hold (ZOH). The continuous system model can be converted to discrete form as (Franklin et al., 1989)

$$x(k+1) = \Phi x(k) + \Gamma u(k) \tag{4.3}$$

$$y(k) = Hx(k) \tag{4.4}$$

where

$$\Phi = e^{FT} = I + FT + \frac{F^2T^2}{2!} + \frac{F^3T^3}{3!} + \ldots \tag{4.5}$$

$$\Gamma = \int_0^T e^{F\eta} d\eta G = \sum_{k=0}^{\infty} \frac{F^k T^{k+1}}{(k+1)!} G \tag{4.6}$$

and where T is the sampling time.

System Controllability and Observability

Observability and controllability are two fundamental system concepts. The observability involves whether the values of the state of the system in the past can be determined by observing the measurements and controllability is concerned with whether or not a control exists that can cause the states of a system to follow some desired path.

For a linear system (equations 4.3 and 4.4) the observability matrix is defined as (Franklin et al., 1989)

$$O = \begin{pmatrix} H \\ H\Phi \\ \cdot \\ \cdot \\ \cdot \\ H\Phi^{N-1} \end{pmatrix} \tag{4.7}$$

and the controllability matrix is defined as

$$C = (\Gamma, \Phi\Gamma, \ldots, \Phi^{N-1}\Gamma) \tag{4.8}$$

A system is observable if and only if the observability matrix is full rank. For a observable system, the states of a system can be observed through measurements and it is also possible to assign estimator poles to any desired positions.

A system is controllable if and only if the controllability matrix is full rank. For a controllable system, it is feasible to assign desired poles of the closed-loop system through state feedback.

Linear Quadratic Gaussian Problem

Consider a controllable and observable linear discrete system

$$x(k+1)=\Phi x(k)+\Gamma u(k)+\Gamma_1 w(k) \tag{4.9}$$

with measurement

$$y(k)=Hx(k)+v(k) \tag{4.10}$$

where w and v are zero mean white process and measurement noises with covariances

$$E(w(k)w^T(k))=R_w\geq 0,\ E(v(k)v^T(k))=R_v\geq 0$$

The LQG problem is to design a state feedback control law u(k)=-Kx(k) which minimizes the cost function

$$J=E(\sum_{k=0}^{N}[x^T(k)Qx(k)+u^T(k)Ru(k)]) \tag{4.11}$$

where the matrices Q, R are symmetric and positive definite.

The solution of the LQG problem is prescribed by the "Separation Principle" (Maciejowski, 1989), which states that the optimal results is achieved by obtaining an estimate state $\hat{x}$ of the state x and then using this estimate as if it were an exact measurement of the state to solve the deterministic linear quadratic control problem. So the LQG can be reduced into two subproblems: state estimation (Kalman filter problem) and state feedback control (LQR problem). The control scheme for LQG control with a LQR and a Kalman filter is shown in Figure 4.1.

Steady-State Linear Quadratic Regulator

The deterministic state equation of equation 4.9 without process noise can be written as

$$x(k+1) = \Phi x(k) + \Gamma u(k) \tag{4.12}$$

Consider controlling the system by feeding back the state x(k) through the gain K as

$$u(k) = -Kx(k) \tag{4.13}$$

The LQR is to chose a state feedback matrix K to minimize the (deterministic) quadratic performance index J

$$J = \sum_{k=0}^{N} \left[x^T(k) Q x(k) + u^T(k) R u(k) \right] \tag{4.14}$$

A block diagram representing the state feedback regulator controller is shown in Figure 4.2. The steady state control rule for this system according to J with N -> ∞ is given by (Franklin et al., 1989)

$$u(k) = -K\,x(k) = -[R+\Gamma^T S\Gamma]^{-1}\Gamma^T S\Phi x(k) \qquad (4.15)$$

where S is the steady state solution to the algebraic Ricatti equation

$$S = \Phi^T[S - S\Gamma(R+\Gamma^T S\Gamma)^{-1}\Gamma^T S]\Phi + Q \qquad (4.16)$$

Kalman Filter

In the LQR, the controller has been designed assuming that all state elements are available. Typically, not all the elements are measured, the missing portion of the states needed to be reconstructed for use in the LQR controller. For the system described by equations 4.9 and 4.10, the optimal states estimation can be achieved through a steady-state Kalman filter. The Kalman filter works as follow:

1. Time update: before the measurement, estimate state $\bar{x}(k)$ without using the measurement y(k)

$$\bar{x}(k) = \Phi\hat{x}(k-1) + \Gamma u(k-1) \qquad (4.17)$$

2. Measurement update: update the estimate $\hat{x}(k)$ from $\bar{x}(k)$ and current measurement y(k) through

$$\hat{x}(k) = \bar{x}(k) + L(k)\,(y(k) - H\bar{x}(k)) \tag{4.18}$$

where L is the steady-state Kalman filter gain

$$L = M H^T (H M H^T + R_v)^{-1} \tag{4.19}$$

and M is the solution of the algebraic Ricatti equation

$$M = \Phi [M - MH^T (HMH^T + R_v)^{-1} HM] \Phi^T + \Gamma_1 R_w \Gamma_1^T \tag{4.20}$$

Figure 4.3 shows the block diagram of a system with a Kalman filter as state estimator.

Sprayer System Analysis

Using equations 4.5 and 4.6, the discrete model that represents the linearized continuous sprayer system of equation 3.23 with gaussian noises can be written as

$$x(k+1) = \Phi x(k) + \Gamma u(k) + \Gamma_d d + \Gamma_1 w(k) \tag{4.21}$$

where

$$x(k) = \begin{pmatrix} q_1(k) \\ q_2(k) \\ p(k) \end{pmatrix}, \quad u(k) = \begin{pmatrix} u_1(k) \\ u_2(k) \end{pmatrix}, \quad d = 1.$$

Define

$$\Gamma_a = (\Gamma : \Gamma_d), \quad u_a(k) = \begin{pmatrix} u(k) \\ d \end{pmatrix}$$

then equation 4.21 can be rewritten as

$$x(k+1) = \Phi x(k) + \Gamma_a u_a(k) + \Gamma_1 w(k) \qquad (4.22)$$

The sprayer system models utilize the 3 states of the two pump net flow rates and boom pressure. The flow rates of the spraying system are usually very low and an accurate flowmeter will cost about 10 times the expense of a pressure transducer. A pressure transducer also has the advantages of quicker response and better reliability. For multi-flow rates control of a sprayer system, the cost of flow meters will be significant. Estimation of pump flow rates through boom pressure measurement can reduce the cost of a spatially-variable control of liquid fertilizer application. Considering the system at steady state, flow rate of a pump (q) can be estimated from input voltage (U) and boom pressure (p) as

$$q = K_{vn} K_{nq} U - (C_1 + K_{pe} K_{vn} K_{nq}) p \qquad (4.23)$$

For pressure measurement, the measurement equation of the linearized discrete model can be written as

$$y(k) = Hx(k) + v \qquad (4.24)$$

with H=(0 0 1) and where v is the measurement noise.

To control the 3th order sprayer system using LQG method, the controllability and observability matrices have to be full

rank (That is of rank 3). Numerical values of models, z plane pole positions, and controllability and observability matrix ranks under different configurations for the spraying system were listed in Table 4.1 for different operating conditions with sample period T=0.0556 sec. These models will also be treated as nominal models and will be used as further design references. It can be seen that the system is controllable and observable under different configurations and that it is possible to apply the LQG technique to control the spraying system.

Variation of Model Parameters

Basically a linearized model can work well only within a limited range about the operating point. The applicable range of the linearized model depends upon how the parameters vary with respect to according to operating condition changes.

Without considering the process noise w(k) and the constant input term caused by linearization in equation 4.21, the system transfer function from input u to state x is

$$T(z) = (zI_{3x3} - \Phi)^{-1}\Gamma \qquad (4.25)$$

The transient characteristic of the system depends majorly upon matrices Φ and Γ. Variations of model parameters at different operating pressures with respect to the nominal models of Table 4.1 were listed in Table 4.2. It can be seen that all the elements' variation are within 5% of the nominal values. The transient characteristic of the system does not

significantly change in the whole working range. It is therefore reasonable to design the LQR controller and Kalman filter using the nominal model for the entire working range.

Closed-Loop Control System Design

In spatially-variable control of spraying systems, the desired fertilizer rates changed step-wise as the applicator travels across the field. Controlling the spraying system with step reference commands, a steady-state control input is necessary to maintain the system at the desired references. Figure 4.4 shows the spraying control block diagram combining a Kalman filter as state observer and a LQR as controller with reference input x_r. When system is at steady state, the steady state reference input u_{ss} can be derived through equation 4.22 as

$$\begin{pmatrix} u_{ss} \\ d \end{pmatrix} = \Gamma_a^{-1} (I_{3\times 3} - \Phi) x_r = F x_r \tag{4.26}$$

The state feedback control law associate with this control scheme system is

$$u(k) = u_{ss} - K(\hat{x}(k) - x_r) \tag{4.27}$$

The over all closed-loop controller of the sprayer system includes two parts: the LQR part and Kalman filter part. According to "Separation Principle" the two parts can be designed separately.

LQR Design

The problem in LQR design is selecting the weighting matrices Q and R. A certain amount of trial and error is usually required (Franklin et al., 1989). Using Bryson and Ho's approach (1969), Q and R can be chosen as diagonal with entries so selected that a fixed percentage change of each variable makes an equal contribution to the cost. The weight between state and control costs can be adjusted according to the control performance by weighing the control cost with a scalar Wc.

For the dual spraying system with 5 D2 nozzle tips, the open-loop control simulation with a step command $x_{r1}=(0,0,0)^T$ to $x_{r2}=(0.008,0.0075,25.86)^T$ is shown in Figure 4.5. The objectives of this spraying system's closed-loop control are

1. To accurately control the steady-state flow rates ratio of the pumps,

2. To improve the transient response of the nozzle flow rate.

The desired steady-state flow rate deviations are of order 0.001 gps while that of boom pressure is of order 1 psi. The state weighting matrix is then chosen as

$$Q=\begin{pmatrix} 1000 & 0 & 0 \\ 0 & 1000 & 0 \\ 0 & 0 & 0.001 \end{pmatrix}$$

The desired steady-state control input deviations are of the same order, so the control weighting matrix can be chosen as

$$R=Wc*\begin{pmatrix}1 & 0\\ 0 & 1\end{pmatrix}$$

where Wc is the scalar control cost weighting compared to the states cost.

To get optimal system responses, simulations of the LQR control with different Wc values were performed using Matlab. When chose Wc=1 was chosen the feedback gain matrix K is

$$K=\begin{pmatrix}0.36 & 0.15 & 0.001\\ 0.1 & 0.41 & 0.0008\end{pmatrix}$$

and the closed-loop poles in the z-domain plane are at 0.16, 0.2555, and 0.8654, which are essentially the same as the open-loop poles listed in Table 4.1. Figure 4.6 shows the simulation results with a step command from x_{r1} to x_{r2}. It can be seen that the system behaves similarly to the open loop because too much weighting factor was put on the control input. Further trials with less weighting on control input has found that for Wc=0.001 the system has quicker nozzle flow rate response while when Wc< 0.001 not much improvement can be achieved. For the case Wc=0.001, the feedback gain

$$K=\begin{pmatrix}87.2 & 19.6 & 0.177\\ 18.8 & 150.1 & 0.22\end{pmatrix}$$

and the closed-loop z-domain poles are at 0.0484, 0.1164, and 0.764. Simulation results for Wc=0.001 were shown in Figure 4.7. The response shows that pump flow rates were high in the transient period in order to improve the transient response of nozzle flow rate. However, the improvement has its limit because of the saturation of power inputs.

Kalman Filter Design

The difference between a general state observer and a steady state Kalman filter is that a Kalman filter is designed based on the knowledge of the noises. To design a Kalman filter, knowledge of the covariance matrices of the process and sensor noises is needed. Covariance of sensor noises R_v can be assigned based on the sensor accuracy. According to the manufacture's specification (New York LTD), the variation of the GP:50 MODEL 211 pressure transducer is about 2% of operating pressure. The measurement noise covariance can then be assigned from the variation of pressure measurement. For example, if a system is operating at 20 psi, the sensor covariance R_v would be 0.16 (psi^2).

Physically, the state noise covariance matrix R_w crudely accounts for unknown disturbances and imperfections of modelling and it is not easy to assign values for on it (Sage and White, 1977). Figure 4.8 shows the typical steady-state pump flow rates and boom pressure responses where the pump flow rates were estimated using equation 4.23. Define X as the state covariance of the estimated steady-state x. At

steady state with constant control inputs, the relationship between X and the process noise covariance R_w can be expressed as a Lyapunov equation (Collins,Jr. and Skelton, 1987)

$$X=\Phi X\Phi^T+\Gamma_1 R_w \Gamma_1^T \tag{4.28}$$

Choosing $\Gamma_1 = I_{3*3}$, R_w can be estimated through the estimated state covariance

$$R_w=X-\Phi X\Phi^T \tag{4.29}$$

Consider that R_w is diagonal, only diagonal terms of the estimated R_w were taken for further design reference. Table 4.3 lists the diagonal terms of the estimated R_w for system with different configurations.

Experimental Results

Equipment for conducting closed-loop control of the dual-pump spraying system were discussed and shown in Figure 3.1. The control procedure using a LQR and a Kalman filter is diagrammed in Figure 4.19. Program "DP.C", in C language, is written for controlling the dual-pump spraying system according to that procedure and is listed in Appendix B.

Effects of Measurement Covariance

Ripple in pump flow rate is a general phenomenon and it would cause the boom pressure oscillations even at steady state. The desired Kalman filter for spraying system control will not only work as state estimator but have to do filter

work to filter out the unwanted pressure ripple. For 5 D2 nozzle tips configuration, the operating pressure is 25.6 psi and the corresponding measurement noise R_v is 0.262 psi^2. With Wc=0.001, the optimal state feedback gain K and Kalman filter gain L could be obtained and listed in Table 4.3 along with the corresponding poles of the LQR and Kalman filter. The experimental results for step references from $(0, 0, 0)^T$ to $(0.008, 0.0075, 25.86)^T$ to $(0.006, 0.005, 13)^T$ to $(0.0095, 0.0085, 34.9)^T$ are shown in Figure 4.9. As can be seen that the system is oscillating at steady state because of the ripple effect. One way to reduce the ripple effect is to design the Kalman filter by assigning a higher measurement noise covariance assuming that the sensor is less accurate than it actually is. The resulting Kalman filter will be less sensitive to noise and the ripple effect will be reduced. Figures 4.10 and 4.11 show the experimental results of Kalman filters designed with measurement noise covariances R_v=2.674 and R_v=10 psi^2. The corresponding Kalman filter gains and poles were listed in Table 4.3. It is clearly that with R_v=10 the system shows better steady state response.

The rule of thumb is to select a estimator responses two to six times faster than the control (Franklin et al., 1989) in order to insure that the system response is dominated by the LQR control. The dominate time constant of the LQR closed-loop system is 0.21 sec. With R_v=10, the estimator time constant is 0.18 which is almost the same as the LQR

control system. With R_v=2.64, the dominate Kalman filter time constant is 0.1 sec which is about two times faster than the LQR control system. In choosing between accuracy of state estimation and reduction of ripple effect, assigning R_v=2.64 to design a Kalman filter will be a good choice for this dual-pump spraying system with 5 D2 nozzle tips configuration.

Results with Different Configurations

Experiments with different system configurations were performed with the Kalman filter designed using the estimated process noise covariance R_w in Table 4.3. The measurement noise covariances R_vs (listed in Table 4.3) were assigned so that the dominate time constants of Kalman filters were less than one-half the dominate response time constants of the LQR control systems. The LQR gains, K, and Kalman filter gains, L, and the corresponding system poles are listed in Table 4.3. Experimental results for different configurations are shown in Figures 4.12 to 4.16.

Closed-Loop and Open-Loop Performance

To compare open-loop and closed-loop performance, experiments with different control schemes were conducted with the 5 D2 nozzle tips configuration. The first control scheme was open-loop control with flow rates estimated using steady-state estimation equation 4.23. The second scheme is closed-loop LQR control with flow rates estimated using the steady-state estimation equation. Both schemes are run with the step reference as Figure 4.10 which shows the experimental results

of closed-loop LQR control with a Kalman filter. The experimental results were shown in Figures 4.17 and 4.18. It can be seen that closed-loop LQR control can reduce the steady-state error caused by model uncertainty and the closed-loop LQR control with a Kalman filter can achieve both reduction of steady-state error and reduction of the ripple effect.

Table 4.1 Numerical Values of Models

Configuration	Φ	$(\Gamma\Gamma_d)$	Poles	O Rank	C Rank
5 D3 Nozzle Tips at 20 psi	0.1453 -1.3302E-2 -1.3068E-4 -7.9254E-3 0.23997 -1.0462E-4 85.643 102.12 0.89163	1.4971E-3 -1.4589E-5 1.8392E-4 -1.2508E-5 1.1222E-3 1.1899E-4 0.19087 0.1388 -1.5335	0.16 0.257 0.859	3	3
3 D3 Nozzle Tips at 35 psi	0.14503 -1.3605E-2 -1.3559E-4 -8.0889E-3 0.23979 -1.0781E-4 88.124 104.92 0.93236	1.4967E-3 -1.4804E-5 1.4881E-4 -1.2679E-5 1.1221E-3 9.6092E-5 0.19406 0.1308 -1.2442	0.16 0.257 0.9	3	3
5 D2 Nozzle Tips at 26 psi	0.14518 -1.3441E-2 -1.3293E-4 -8E-3 0.23989 -1.0609E-4 86.782 103.4 0.91026	1.4969E-3 -1.4688E-5 1.7976E-4 -1.2586E-5 1.1221E-3 1.162E-4 0.19234 0.13589 -1.5007	0.16 0.257 0.878	3	3
3 D2 Nozzle Tips at 40 psi	0.14498 -1.3658E-2 -1.3644E-4 -8.1172E-3 0.23976 -1.0837E-4 88.556 105.4 0.9395	1.4967E-3 -1.4841E-5 1.36E-4 -1.2708E-5 1.1221E-3 8.7785E-5 0.19462 0.13746 -1.1376	0.16 0.257 0.907	3	3
5 XR3 Nozzle Tips at 18 psi	0.14539 -1.32E-2 -1.2904E-4 -7.8704E-3 0.24 -1.0356E-4 84.811 101.18 0.87807	1.4972E-3 -1.4517E-5 1.9414E-4 -1.245E-5 1.1222E-3 1.2569E-4 0.18979 0.13414 -1.6171	0.16 0.257 0.866	3	3
3 XR3 Nozzle Tips at 30 psi	0.14508 -1.3551E-2 -1.347E-4 -8.0595E-3 0.23982 -1.0724E-4 87.678 104.41 0.925	1.4968E-3 -1.4765E-5 1.5414E-4 -1.2648E-5 1.1221E-3 9.9569E-5 0.19349 0.13668 -1.2881	0.016 0.257 0.893	3	3

Table 4.2 Parameter Variations of Models

Configuration	$\delta\Phi_{ij}/\Phi_{ij}$	$(\delta\Gamma_{ij}/\Gamma_{ij}; \delta\Gamma_{dij}/\Gamma_{ij})$
5 D3 Nozzle Tips at 38 psi	-9.4E-4 1.1E-2 1.9E-2 1E-2 -3.8E-4 1.5E-2 1.4E-2 1.37E-2 2.3E-2	-1E-5 7.4E-3 0.39 6.9E-3 -5.2E-5 0.39 8.4E-3 8.2E-3 0.4
5 D3 Nozzle Tips at 9 psi	1.6E-3 -2E-2 -3.3E-2 -1.8E-2 6.6E-4 -2.7E-2 -2.5E-2 -2.4E-2 -4E-2	1.8E-4 -1.3E-2 -0.34 -1.2E-2 9.2E-5 -0.34 -1.5E-2 -1.4E-2 -0.34
3 D3 Nozzle Tips at 55 psi	-3.3E-4 3.9E-3 6.3E-3 3.5E-3 -1.3E-4 5.2E-3 4.9E-3 4.7E-3 7.7E-3	-3.6E-5 2.5E-3 0.26 2.3E-3 -1.8E-5 0.26 2.9E-3 2.8E-3 0.26
3 D3 Nozzle Tips at 18 psi	6E-4 -7.1E-3 -1.1E-2 -6.4E-3 2.4E-4 -9.4E-3 -9E-3 -8.5E-3 -1.4E-2	6.6E-5 -4.6E-3 -0.28 -4.3E-2 3.3E-5 -0.28 -5.2E-3 -5.1E-3 -0.28
5 D2 Nozzle Tips at 42 psi	-5.6E-4 6.7E-3 1.1E-2 6.1E-3 -2.2E-4 8.9E-3 8.5E-3 8.1E-3 1.3E-2	-6.2E-5 4.3E-3 0.28 4E-3 -3.1E-5 0.28 4.9E-3 4.8E-3 0.29
5 D2 Nozzle Tips at 13 psi	1.1E-3 -1.3E-2 -2.1E-2 -1.2E-2 4.3E-4 -1.7E-2 -1.6E-2 -1.5E-2 -2.5E-2	1.2E-4 -8.2E-4 -0.3 -7.7E-2 5.9E-5 -0.3 -9.4E-3 -9.1E-3 -0.3
3 D2 Nozzle Tips at 64 psi	-2.6E-4 3.1E-3 5.1E-3 2.8E-3 -1.1E-4 4.1E-3 3.9E-3 3.7E-3 6.1E-3	-2.9E-5 2E-3 0.27 1.9E-3 -1.4E-5 0.27 2.3E-3 2.2E-3 0.27
3 D2 Nozzle Tips at 19 psi	5.6E-4 -6.6E-3 -1.1E-2 -6E-3 2.2E-4 -8.7E-3 -8.3E-3 -7.9E-3 -1.3E-2	6.2E-5 -4.3E-3 -0.31 -4E-3 3.1E-5 -0.31 -4.8E-3 -4.7E-3 -0.31
5 XR3 Nozzle Tips at 34 psi	-1.1E-3 1.3E-2 2.2E-2 1.2E-2 -4.4E-4 1.8E-2 1.7E-2 1.6E-2 2.7E-2	-1.2E-4 8.6E-3 0.39 8E-3 -6E-5 0.38 9.8E-3 9.5E-3 0.39
5 XR3 Nozzle Tips at 8 psi	1.9E-3 -2.3E-2 -3.8E-2 -2.1E-2 7.6E-4 -3.1E-2 -2.9E-2 -2.7E-2 -4.5E-2	2.1E-4 -1.5E-2 -0.34 -1.4E-2 1E-4 -0.34 -1.7E-2 -1.6E-2 -0.34
3 XR3 Nozzle Tips at 50 psi	-4.3E-4 5.1E-3 8.3E-3 4.6E-3 -1.7E-4 6.8E-3 6.5E-3 6.1E-3 1E-2	-4.8E-5 3.3E-3 0.29 3.1E-3 -2.4E-5 0.29 3.8E-3 3.7E-3 0.29
3 XR3 Nozzle Tips at 14 psi	8.8E-4 -1.1E-2 -1.7E-2 -9.6E-3 3.6E-4 -1.4E-2 -1.3E-2 -1.3E-2 -2.1E-2	9.8E-5 -6.8E-3 -0.32 -6.4E-3 4.9E-5 -0.32 -7.8E-3 -7.6E-3 -0.33

Table 4.3 Parameters Used in LQG Control for Different Configurations

Configuration (Experimental Results)	Kalman Filter Parameters				LQR Parameter		Step References in Experiment (x_{r1}-x_{r2}-x_{r3})
	Diagonal terms of Estimated R_w	R_v	L	Poles	K^T	Poles	
5 D2 Tips (Fig 4.9)	1.24E-8 7.2E-9 0.6	0.264	-2.31E-5 -1.92E-5 0.74	0.18 0.23+0.051i 0.23-0.051i	88.6 19.63 21 150 0.195 0.228	0.048 0.111 0.767	8E-3 6E-3 9.5E-3 7.5E-3 5E-5 8.5E-3 25.86 13 34.9
5 D2 Tips (Fig 4.11)	1.24E-8 7.2E-9 0.6	10	-1.71E-5 -1.49E-5 0.154	0.16 0.258 0.739	88.6 19.63 21 150 0.195 0.228	0.048 0.111 0.767	8E-3 6E-3 9.5E-3 7.5E-3 5E-5 8.5E-3 25.86 13 34.9
5 D2 Tips (Fig 4.10)	1.24E-8 7.2E-9 0.6	2.64	-2.84E-5 -2.4E-5 0.328	0.16 0.26 0.58	88.6 19.63 21 150 0.195 0.228	0.048 0.111 0.767	8E-3 6E-3 9.5E-3 7.5E-3 5E-5 8.5E-3 25.86 13 34.9
3 D2 Tips (Fig 4.12)	8.53E-9 1.6E-9 0.41	1.92	-3E-5 -2.17E-5 0.335	0.16 0.258 0.6	91.6 23 24.6 154.4 0.232 0.27	0.048 0.116 0.775	6E-3 4.5E-3 7.5E-3 5.5E-3 3.7E-5 6.5E-3 39.5 20.1 58.6
5 D3 Tips (Fig 4.13)	9.38E-9 5.42E-9 0.45	1.91	-2.74E-5 -2.33E-5 0.33	0.16 0.26 0.567	86.9 17.7 18.8 147.7 0.173 0.204	0.048 0.11 0.76	8.2E-3 5.5E-3 1E-2 7.8E-3 4.5E-5 9.5E-3 20 7.8 29.6
3 D3 Tips (Fig 4.14)	1E-8 1.83E-8 0.5	2.2	-3.05E-5 -2.15E-5 0.34	0.16 0.258 0.589	90.8 22.1 23.7 153.1 0.223 0.259	0.048 0.116 0.774	6.7E-3 5E-3 8.5E-3 6E-3 4E-5 6.8E-3 34.9 17.5 50.6
5 XR3 Tips (Fig 4.15)	1.01E-8 5.89E-9 0.49	1.9	-2.69E-5 -2.29E-5 0.336	0.16 0.268 0.55	85.8 16.4 17.4 146.1 0.159 0.187	0.048 0.111 0.757	9E-3 6.5E-3 1.1E-2 8E-3 5E-5 9.5E-3 17.84 8.2 26
3 XR3 Tips (Fig 4.16)	1.27E-8 7.37E-9 0.62	2.23	-3.1E-5 -2.6E-5 0.368	0.16 0.26 0.553	90 21.3 22.7 152 0.213 0.249	0.048 0.111 0.77	7E-3 5E-3 8.5E-3 6.2E-3 4E-5 8E-3 29.9 13.9 46.7

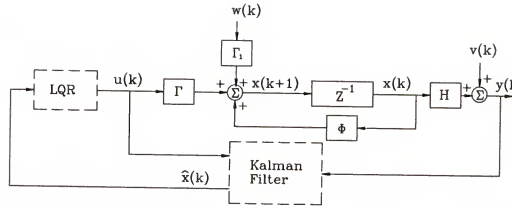

Figure 4.1 Control Scheme with a LQR and a Kalman Filter.

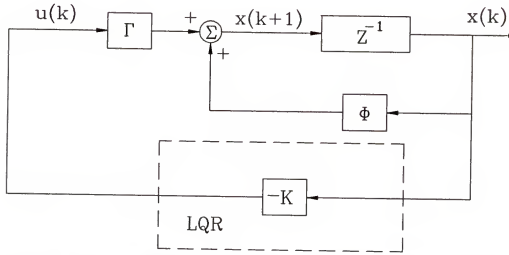

Figure 4.2 Closed-Loop Control with a Linear Quadratic Controller.

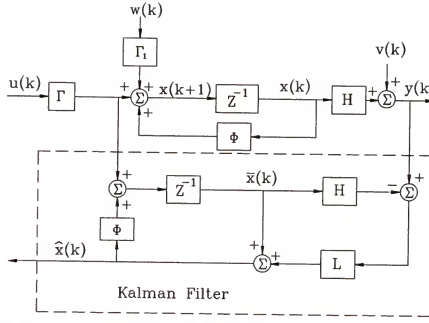

Figure 4.3 Block Diagram of Kalman Filter.

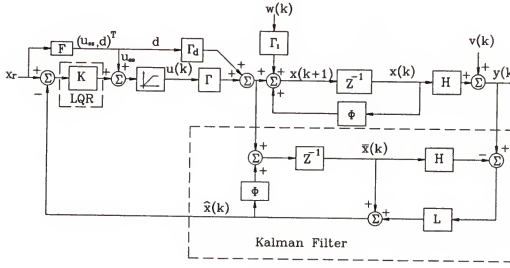

Figure 4.4 Block Diagram of LQG Closed-Loop Control of Spraying System.

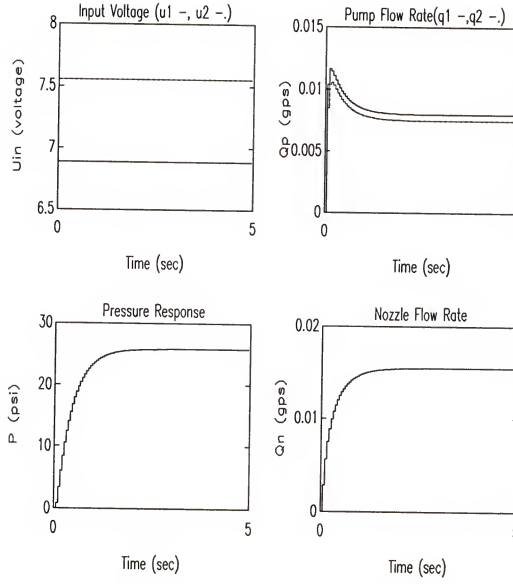

Figure 4.5 Simulation of Open-Loop Step Responses for 5 D2 Nozzle Tips Configuration and $x_r=(0.008,0.0075,25.86)^T$.

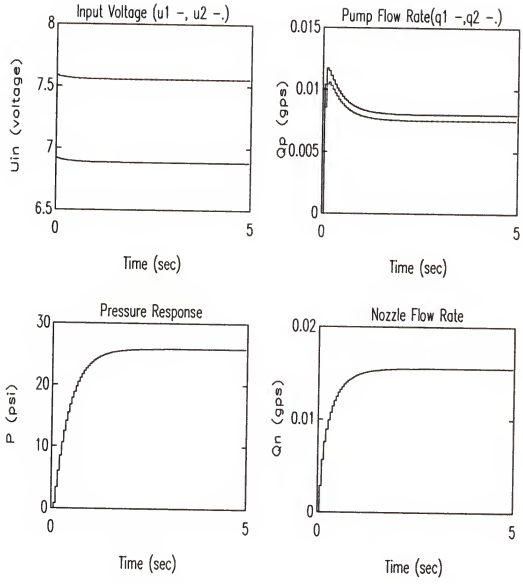

Figure 4.6 Simulation of LQR control for Wc=1 and $x_r=(0.008,0.0075,25.86)^T$ (5 D2 Nozzle Tips Configuration).

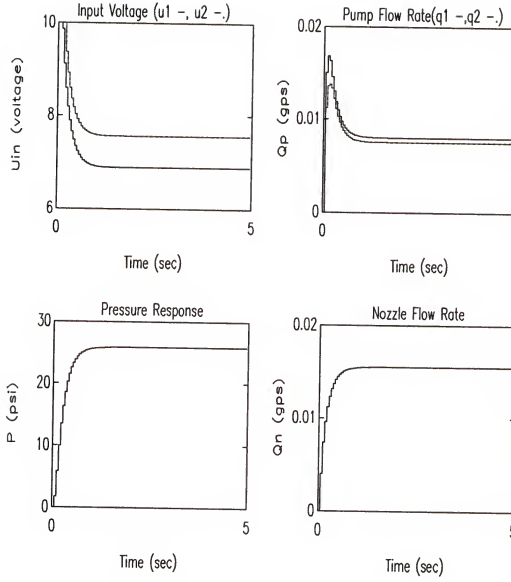

Figure 4.7 Simulation of LQR Control with Wc=0.001 and $x_r=(0.008,0.0075,25.86)^T$ (5 D2 Nozzle Tips Configuration).

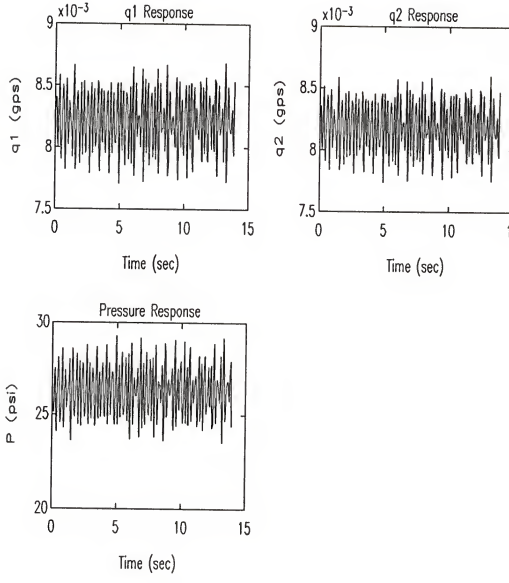

Figure 4.8 Typical Flow Rates and Pressure Steady-State Responses.

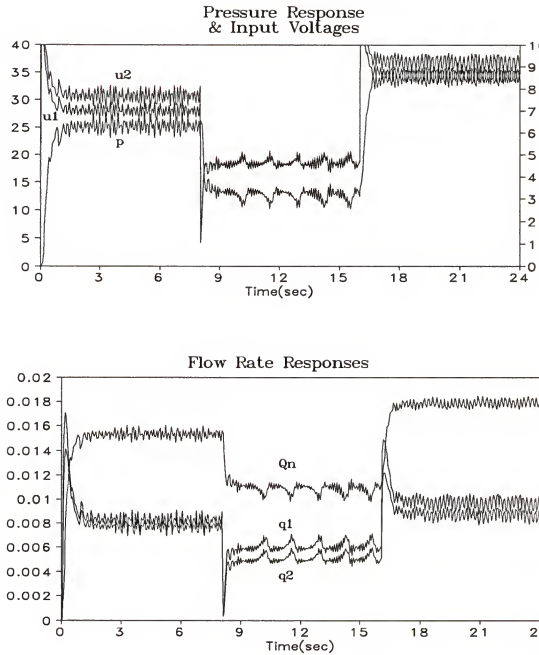

Figure 4.9 LQG Control Experimental Results of 5 D2 Nozzle Tips Case with R_v=0.264 psi^2.

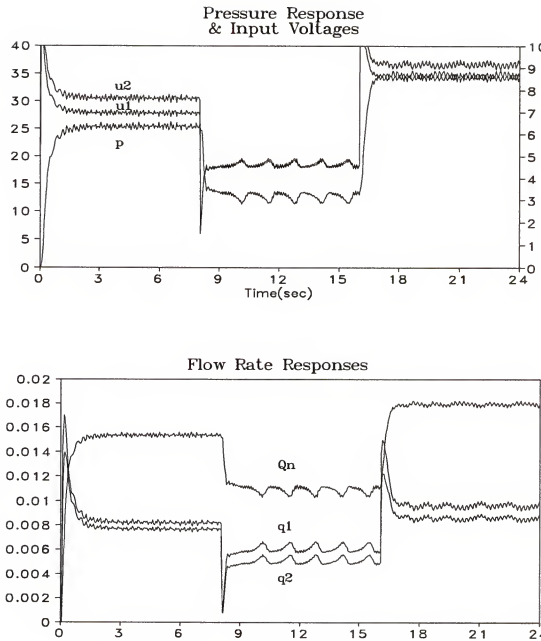

Figure 4.10 LQG Control Experimental Results of 5 D2 Nozzle Tips Case with R_v=2.64 psi^2.

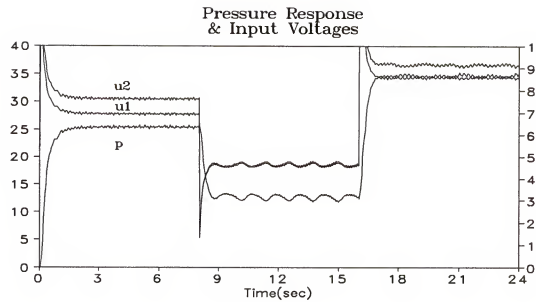

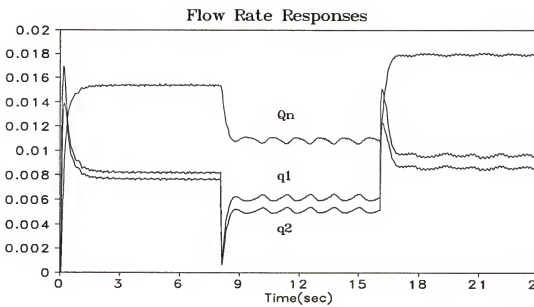

Figure 4.11 LQG Control Experimental Results of 5 D2 Nozzle Tips Case with R_v=10 psi^2.

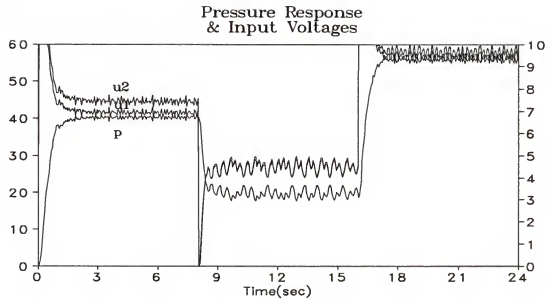

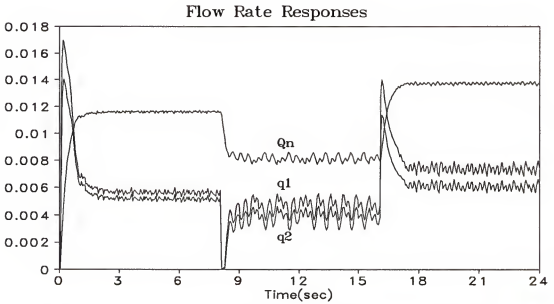

Figure 4.12 LQG Control Experimental Results of 3 D2 Nozzle Tips Case with R_v=1.92 psi^2.

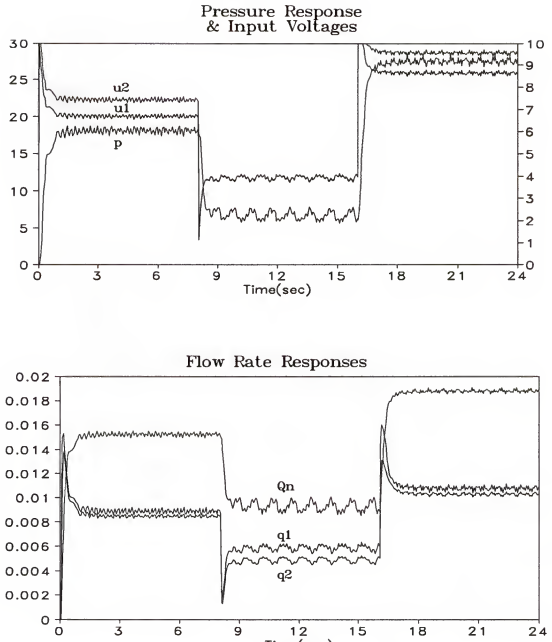

Figure 4.13 LQG Control Experimental Results of 5 D3 Nozzle Tips Case with R_v=1.91 psi^2.

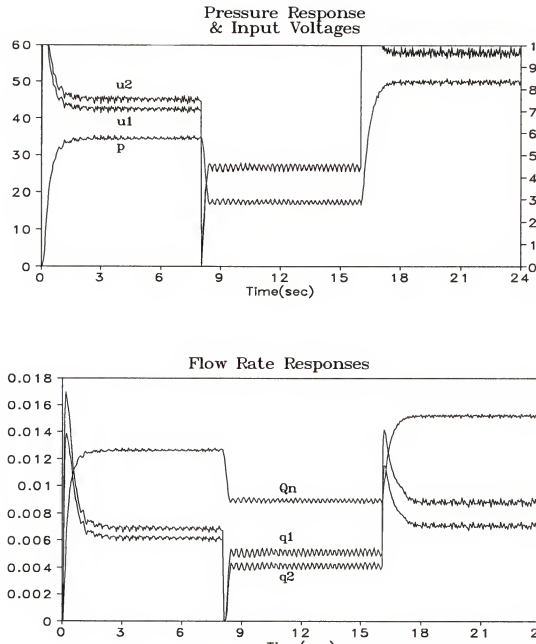

Figure 4.14 LQG Control Experimental Results of 3 D3 Nozzle Tips Case with R_v=0.22 psi^2.

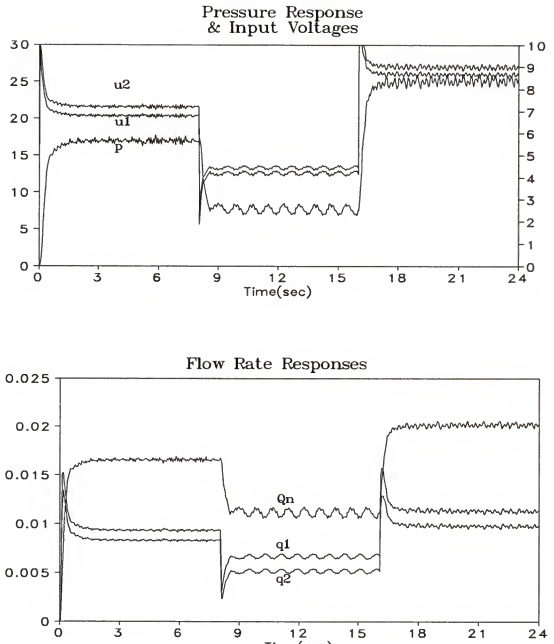

Figure 4.15 LQG Control Experimental Results of 5 XR3 Nozzle Tips Case with R_v=1.9 psi^2.

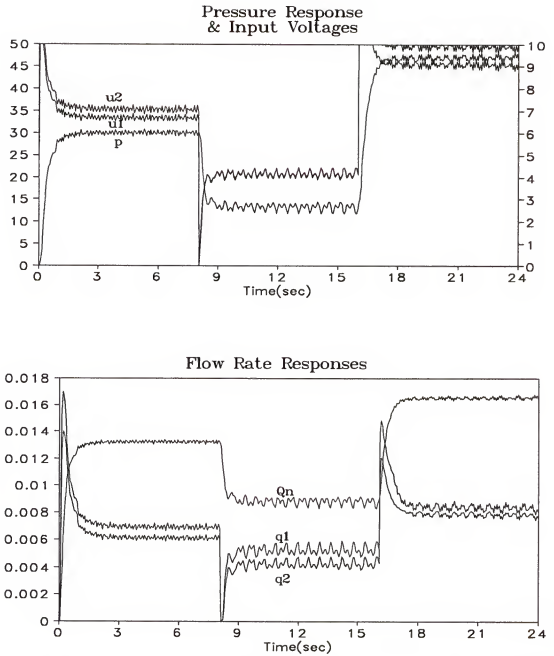

Figure 4.16 LQG Control Experimental Results of 3 XR3 Nozzle Tips Case with R_v=2.23 psi^2.

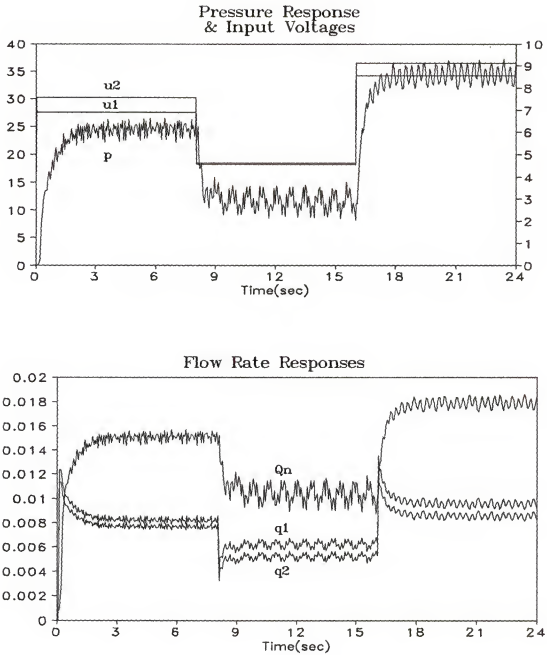

Figure 4.17 Open-Loop Control Experimental Results of 5 D2 Nozzle Tips Case.

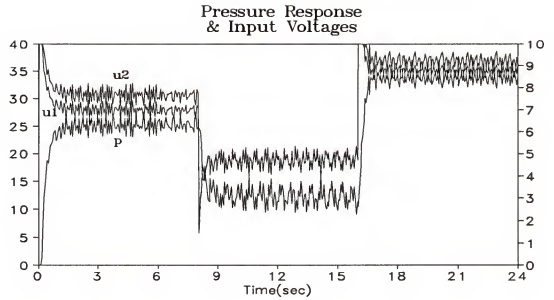

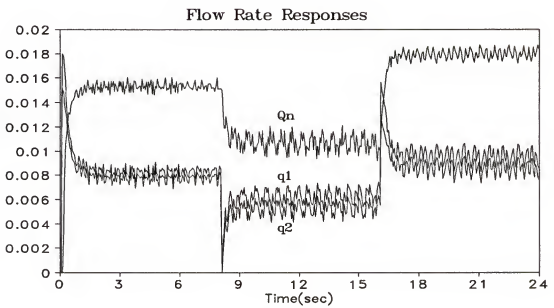

Figure 4.18 LQR (without Kalman Filter) Control Experimental Results of 5 D2 Nozzle Tips Case.

1. Initialize data acquisition board.
2. Input desired flow rates x_r.
3. Calculate steady-state feedforward commands.

$$\begin{pmatrix} u_{ss} \\ d \end{pmatrix} = \Gamma_a^{-1}(I_{3*3} - \Phi)x_r = Fx_r$$

4. Initialize state x(0) and input u(0).
5. Start control loop:
6. Time update.

$$\bar{x}(k) = \Phi \hat{x}(k-1) + \Gamma u(k-1)$$

7. Measure boom hose pressure y(k) from A/D.
8. Measurement update.

$$\hat{x}(k) = \bar{x}(k) + L(\, y(k) - H\bar{x}(k)\,)$$

9. Calculate input command.

$$u(k) = u_{ss} - K(\, \hat{x}(k) - x_r\,)$$

10. Write command to D/A.
11. Wait for end of sample period.
12. Go to 5.

Figure 4.19 Control Process.

CHAPTER 5
SELECTION OF BOOM HOSE DIAMETER

Introduction

The diameter of the boom hose has two important impacts on the fertilizer application: flow distribution along the boom and transportation delay time from the pump to each nozzle. The flow rate through each nozzle depends on the pressure difference across it. Since sprayers are vented to atmosphere, the flowrate through a nozzle depends upon the upstream pressure. In general the boom hose was historically designed with a large internal diameter to eliminate flow pressure losses and therefore make the pressure distribution in the boom uniform and the flow rates of the nozzles equal. This is a sensible design for separated-mixture spraying systems, but not for combined-mixture ones in which the sprayed material ratio is to be changed. The problem is that a long time is needed for the new mixture to reach the far end nozzle. When a mixture concentration ratio is changed, the nozzle nearest the fluid entrance will soon spray mixture with the new mixture ratio while the farthest end nozzle will still spray the previous mixture with the old ratio until the new mixture reaches this nozzle. The transportation delay can be compensated for by a precommand. However, a procedure is then needed to compute the best precommand. Both of these problems

will be discussed in this chapter and computer programs for selecting a best boom hose diameter size and best precommand time will be developed.

Flow Distribution in the Boom

A sprayer boom is essential a flow dividing manifold with nozzles positioned laterally. Figure 5.1 shows the structure of a dividing manifold. The distribution of flow out of the manifold is determined by the momentum and friction of the flow. From nozzle to nozzle, fluid pressure is lost because of the wall friction. When portion of the fluid is sprayed out of nozzle the remaining fluid will decelerate in a uniform diameter manifold and the pressure will be higher from the regain of momentum. Previous research (Bralt, 1985; Perold, 1977; Wu and Gitlin, 1974; Ahmad, 1981) in the similar problem of flow distribution in irrigation pipes have used the Bernoulli equation to study this problem. By assuming continuous flow sprayed out a slot Ahmad (1981) found that selecting the diameter d (m), length of boom L (m), and the friction factor f such

$$\frac{fL}{3d}=1$$

will minimize the pressure variation.

Bajura and Jones (1976) has pointed out that the difficulty with applying a Bernoulli equation to the branching process lies in the ambiguity which exists in identifying a

relevant streaming on which to conserve energy and estimate frictional loss. The momentum balance for the axial direction of the control volume in Figure 5.1 is (Pigford et al., 1983)

$$(\rho u_1 S)\, u_1 - (\rho u_2 S)\, u_2 = (p_2 - p_1)\, S \qquad (5.1)$$

where S is the cross sectional area of the hose. The above equation is based on the assumption that all the momentum loss has recovered from pressure acting in the boom cross section. In fact, some of fluid will retain part of its initial forward momentum as it crosses the control surface and leaves the boom. Considering the momentum lost due to the flow leaving the boom, equation 5.1 should be modified with a coefficient k and becomes (Pigford et al., 1983)

$$p_2 - p_1 = k\rho\,(u_1^2 - u_2^2) \qquad (5.2)$$

The coefficient k usually is determined by experiment. Pigford et al. indicated that few measurements of k have been published, the most complete analysis of existing data appears to be that of Millers (1971). Pigford et al. had converted Millers' experimental results into their coefficients k in the above equation and found that k ranged from 0.4 to 0.5.

The pressure lose between nozzles is due to friction and can be written as

$$\Delta p_f = \rho f \frac{L}{d} \frac{V^2}{2} \tag{5.3}$$

where ρ is the fluid density, L is the length between nozzles, d is the pipe diameter, and V is the flow mean velocity. For a smooth pipe the friction coefficient is (Massey, 1983)

$$f = \frac{16}{R_e} \qquad for \ R_e < 2000$$

$$f = 0.001375 + 0.1375 R_e^{-\frac{1}{3}} \qquad for \ R_e > 2000$$

$$R_e = \frac{Vdp}{\mu} \quad , \mu = fluid\ viscosity\ coefficient$$

From Figure 5.2, the pressure difference between nozzle n and n+1 is

$$p_n' - p_{n+1} = \rho f \frac{L}{d} \frac{u^2_{n+1}}{2} \tag{5.4}$$

The pressure difference after and before nozzle n is

$$p_n' - p_n = k\rho (u^2_n - u^2_{n+1}) \tag{5.5}$$

The pressure at nozzle can then be approximated as the average pressure of p_n and p'_n and the flow rate of the nozzle can be written as

$$q_n = C_d \sqrt{\frac{p_n' + p_n}{2}} \tag{5.6}$$

Substituting for p'_n using equation 5.5, equation 5.6 can be rewritten as

$$\begin{aligned} q_n &= C_d\sqrt{p_n + \frac{k\rho}{2}(u_n^2 - u_{n+1}^2)} \\ &= C_d\sqrt{p_n + \frac{k\rho}{2}\left(\frac{4}{\pi d^2}\right)^2 (Q^2 - (Q - q_n)^2)} \\ &= C_d\sqrt{p_n + K_1(2Qq_n - q_n^2)} \end{aligned} \tag{5.7}$$

where

$$K_1 = \frac{8k\rho}{\pi^2 d^4}$$

From equation 5.7, nozzle flow rate q_n can be solved as

$$q_n = \frac{C_d^2 K_1 Q \pm C_d\sqrt{(C_d K_1 Q)^2 + p_n(1 + K_1 C_d^2)}}{1 + C_d^2 K_1} \tag{5.8}$$

Since the nozzle flow rate must be positive, the feasible value of q_n is

$$q_n = \frac{C_d^2 K_1 Q + C_d\sqrt{(C_d K_1 Q)^2 + p_n(1 + K_1 C_d^2)}}{1 + C_d^2 K_1} \tag{5.9}$$

Application Errors

Nonuniform flow distribution along the boom is not the only source of application errors. Two other error sources

are the dynamic response of nozzle flow rate and the transportation delay of flow.

Dynamic Response

The typical nozzle flow response of simple sprayer systems can be simplified as a first order systems with a time constant τ and a steady state gain K (Wang, 1991). If control starts with no fluid in the boom, the fluid will need to fill the volume of boom and then begin to build up boom pressure, and therefore nozzle flow rate. In this case there will be a delay time D and the transfer function for nozzle flow rate Q_n as a function of desired nozzle flow rate Q_d can be written as

$$\frac{Q_n(s)}{Q_d(s)} = \frac{Ke^{-Ds}}{\tau s+1} \tag{5.10}$$

where

$$D = \frac{V}{Q}$$

where V is the total system volume, from outlet of pump to the end of boom and Q is the pump flow rate. In spatially-variable application, the boom will be filled with fluid except during first step command from zero flow. Hence there is no delay time D and the boom pressure and nozzle flow rate will response quickly as the command is changed. In this case the transfer function can be expressed as

$$\frac{Q_n(s)}{Q_d(s)} = \frac{K}{\tau s+1} \qquad (5.11)$$

Assuming that there is no steady-state error, nozzle flow response to a step command can be shown as in Figure 5.3. The application error here is defined as the difference between the desired flow rate and the actual nozzle flow rate.

Transportation Delay

Sprayer systems are usually configured with multiple nozzles. Figure 5.4 shows the alignments of the nozzles for systems with even number and odd number of total nozzles with fluid injected into the boom at middle of the boom. When desired nozzle flow rate is changed, nozzle flow rate will change according equation 5.11 for separated-mixture spraying systems. For combined-mixture spraying systems, if the concentration ratio of mixture is changed, the nozzle will spray out the same old mixture till the new mixture arrives. Figure 5.5 shows a example of application error caused by transportation delay when desired flowrate changed from Q_1 (mixture A) to Q_2 (mixture B).

Assuming that the flow is plug flow, the transportation delay (T_i) of nozzle flow is the travelling time that fluid needs to travel from the outlet of pump to the i^{th} nozzle. Define (t_h) as the fluid travelling time through header (hose from pump outlet to injection spot of boom) and

$$t_h = \frac{A_h l_h / 2}{Q/2} = \frac{A_h l_h}{Q} \tag{5.12}$$

For an even total nozzles configuration system, the delay for nozzle 1 is

$$T_1 = t_h + \frac{Al/2}{Q/2} = t_h + \frac{Al}{Q} \tag{5.13}$$

and for the other nozzles is

$$T_i = \sum_{j=1}^{i-1} T_j + \frac{Al}{\frac{Q}{2} - \sum_{j=1}^{i-1} q_{nj}} \tag{5.14}$$

where

A = cross area of boom, $0.25\pi d^2$,

A_h =cross area of header, $0.25\pi d_h^2$,

Q = pump flow rate,

l = distance between nozzles,

d_h = header hose diameter,

l_h = header length,

q_{ni} = i^{th} nozzle flow rate.

For an odd total nozzle configuration case, delay for nozzle 0 is t_h, for nozzle 1 is

$$T_1 = t_h + \frac{2Al}{Q - q_{no}} \tag{5.15}$$

and for other nozzles is

$$T_i = \sum_{j=1}^{i-1} T_j + \frac{Al}{\frac{Q - q_{n0}}{2} - \sum_{j=1}^{i-1} q_{nj}} \qquad (5.16)$$

Application Error Formulation

In spatially-variable application, the desired application rate changes when the applicator travels into zones with different desired application rates. The application rate usually changes stepwise (either step-up or step-down). Assume that applicator changes command every t_{cell} seconds and a precommand time t_c is used to compensate for the application errors from dynamic response and transportation delays to the nozzles. As an application rate changing example, consider the application rates and mixture contents changing from $Q0_d$ gpm (mixture A) to Q_d gpm (mixture B) to $Q0_d$ gpm (mixture B) during an application with a time constant τ seconds during t_{cell} periods. The problem of determining the application errors caused by nonuniform flow distribution and transportation delay in a t_{cell} period can classified into two different cases according to nozzle's delay time.

Case A involves nozzles with time delay (T_i) longer than precommand time(t_c). Figure 5.6 shows the error caused in case A. Define that MCR as the mixture changing ratio from mixture A to mixture B, for example, if mixture A and mixture B have the same material concentration then MCR is 0, and if

A and B are of totally different materials then MCR is 1. The mixture sprayed between t_c and T_i after command changed (heavier hatched area in Figure 5.6) consists of MCR portion of unnecessary material and (1-MCR) portion of desired material. The application error caused by transportation delay during this period can be written as

$$E_d = MCR \int_{t_c}^{T_i} (q_n + (q0_n - q_n)\, e^{-\frac{t}{\tau}})\, dt + \int_{t_c}^{T_i} \left| ((1-MCR)(q_n + (q0_n - q_n)\, e^{-\frac{t}{\tau}}) - Q_d) \right| dt \tag{5.17}$$

The first term of E_d is the error caused by applying unnecessary material and the second term is the integral absolute error (Ogata, 1990) between desired application rate Q_d and actual applied rate. The overall integral absolute application error for case A can be formulated as

$$Err = E_d + \int_{T_i}^{t_{cell}} \left| (q_n + (q0_n - q_n)\, e^{-\frac{t}{\tau}} - Q_d) \right| dt + \int_{0}^{t_c} \left| (q0_n + (q_n - q0_n)\, e^{-\frac{t}{\tau}} - Q_d) \right| dt \tag{5.18}$$

Case B includes when $T_i < t_c$ (Figure 5.7). The integral absolute error can be written as

$$
\begin{aligned}
Err = & \int_{t_c}^{t_{cell}} \left| (Q_d - (q_n + (q0_n - q_n)\, e^{-\frac{t}{\tau}}) \right| dt \\
& + \int_{0}^{T0_i} \left| (q0_n + (q_n - q0_n)\, e^{-\frac{t}{\tau}} - Q_d) \right| dt \\
& + \int_{T0_i}^{t_c} \left| (Q_d - (1 - MCR)\,(q0_n + (q_n - q0_n)\, e^{-\frac{t}{\tau}})) \right| dt \\
& + MCR \int_{T0_i}^{t_c} (q0_n + (q_n - q0_n)\, e^{-\frac{t}{\tau}})\, dt
\end{aligned}
\tag{5.19}
$$

For a step-down example, case A involves nozzles with time delay ($T0_i$) longer than precommand time(t_c). The application error of case A (Figure 5.8) can be formulated as

$$
\begin{aligned}
Err0 = & MCR * \int_{t_c}^{T0_i} (q0_n + (q_n - q0_n)\, e^{-\frac{t}{\tau}})\, dt \\
& + \int_{t_c}^{T0_i} \left| ((1 - MCR)\,(q0_n + (q_n - q0_n)\, e^{-\frac{t}{\tau}}) - Q0_d) \right| dt \\
& + \int_{T0_i}^{t_{cell}} \left| (q0_n + (q_n - q0_n)\, e^{-\frac{t}{\tau}} - Q0_d) \right| dt \\
& + \int_{0}^{t_c} \left| (q_n + (q0_n - q_n)\, e^{-\frac{t}{\tau}} - Q0_d) \right| dt
\end{aligned}
\tag{5.20}
$$

Case B occurs when $T0_i < t_c$ (Figure 5.9). The integral absolute error can be written as

$$
\begin{aligned}
Err0 = & \int_{t_c}^{t_{cell}} \left| \left(q0_n + \left(q_n - q0_n\right) e^{-\frac{t}{\tau}} - Q0_d\right) \right| dt \\
& + \int_{0}^{T_1} \left| \left(q_n + \left(q0_n - q_n\right) e^{-\frac{t}{\tau}} - Q0_d\right) \right| dt \\
& + MCR \int_{T_1}^{t_c} \left(q_n + \left(q0_n - q_n\right) e^{-\frac{t}{\tau}}\right) dt \\
& + \int_{T_1}^{t_c} \left| \left((1 - MCR) \left(q_n + \left(q0_n - q_n\right) e^{-\frac{t}{\tau}}\right) - Q0_d\right) \right| dt
\end{aligned}
\qquad (5.21)
$$

The total integral absolute application error (E) for a period of step-up and stp-down command changing is the sum of all errors across nozzles

$$E = 2 \sum_{i=1}^{\frac{N}{2}} \left(Err_i + Err0_i\right) \quad \textit{for N is even}$$

$$E = Err_0 + Err0_0 + 2 \sum_{i=1}^{\frac{N-1}{2}} \left(Err_i + Err0_i\right) \quad \textit{for N is odd}$$

The sprayer boom hose diameter and precommand time of a combined-mixture system could therefore be selected to minimize total integral absolute error E.

Separated-Mixture System Application Error

The application error of a separated-mixture system mainly depends on system dynamic response since there is no material changing and it is usually designed to achieve uniform flow distribution. For a separated-mixture system with uniform flow distribution, the application error during

t_{cell} period for each nozzle can be shown in Figure 5.10 and formulated as

$$\begin{aligned} E_s &= \int_{t_c}^{t_{cell}} (Q_d - (Q0_d + (Q_d - Q0_d)(1 - e^{-\frac{t}{\tau}}))) dt \\ &+ \int_{0}^{t_c} (Q_d - (Q_d + (Q0_d - Q_d)(1 - e^{-\frac{t}{\tau}}))) dt \\ &= (Q_d - Q0_d)(t_c - \tau - \tau e^{-\frac{t_{cell}}{\tau}} + 2\tau e^{-\frac{t_c}{\tau}}) \end{aligned} \tag{5.22}$$

The minimum occurs when

$$\frac{d E_s}{dt_c} = (Q_d - Q0_d)(1 - 2e^{-\frac{t_c}{\tau}}) = 0$$

which is optimal precommand time $t_c = 0.693\tau$.

Optimal Diameter and Precommand Time

The overall application error of combined-mixture type spraying systems can be formulated by combining the errors caused by nonuniform flow distribution, dynamic response, and transportation delay. To minimize application error caused by nonuniform flow distribution, the boom diameter should be designed as big as possible. To minimize the application error caused by transportation delay and system dynamics, the boom diameter should be as small as possible so that the system will response quickly and the nozzle delay time will be reduced. To minimize the total integral absolute application error (E) caused by these factors, a optimal boom diameter (d)

and a best precommand time (t_c) have to be selected subject to the bounds on reasonableness of

1. 0.125" <= d <= 1.5"

2. 0 <= t_c <= t_{cell}.

A computer program for determining the optimal boom diameter (d) and optimal precommand time (t_c) was written using the Powell Searching and the Golden Section methods (Vanderplaats, 1971) and it is listed in Appendix A. The inputs to the program describe the configuration of spraying system (total number of nozzles, distance between nozzles, discharge coefficient, total flow rates, mixture changing ratio (MCR), and k of equation 5.5) and the outputs are the optimal diameter d, optimal precommand time t_c, minimum application error, and the flow rates, pressures, and delay times of each nozzle.

Test Cases

Both odd and even number nozzle cases were tested, Test cases with a system with 12 nozzles was conducted and the sprayer configuration is listed in Table 5.1. The results were shown in Tables 5.2 and 5.3. Figure 5.11 shows the application errors versus boom diameter with fixed precommand times and Figure 5.12 shows the application errors versus precommand time with fixed boom diameters for 12 nozzle case. Figure 5.13 shows the application error and its contour as function of both d and t_c. The minimum occurs at a boom hose

diameter of 0.43" and a precommand time of 0.625 seconds using Powell searching method.

Mixture Changing Ratio

In the previous test cases, the MCR was assumed to be 0.5 and the application errors are 8.8% and 9.2% of average application rate for 12 and 13 nozzles cases. MCR value changes with field conditions. Table 5.4 shows the optimal design results of 12 nozzle case with different MCR values. It can be seen that the error percentage drops as MCR decreases and the combined-mixture spraying system works like separated-mixture system when MCR is 0. The separated-mixture system has less application error (6.2%) than the combined-mixture system (> 6.8%).

Cell Size Effect

In spatially-variable application, a field was divided into cells according field variability. Optimal boom diameter selection also depends on the cell size. Table 5.5 shows results of different cell sizes for the 12 nozzle test case. It can be seen that the application error to average application rate decreases when cell size increases. Also, the smaller the cell size the more significant the error caused by transportation delay which therefore results in a smaller boom hose diameter. On the contrary, more on uniform flow distribution is emphasized with a large cell size.

System Dynamic Effect

The dynamic response effect on application error can be seen in Figure 5.3. For separated-mixture systems with uniformly flow distribution, transportation delays will not affect application error since the mixture concentration ratios are the same before and after a command change. Table 5.4 shows this fact that optimal design of separated-mixture system (MCR=0) tends to have a large boom hose diameter and its precommand time 0.7 seconds is about 0.693 times the system time constant. Consider the 12 nozzle test case as a separated-mixture system with boom diameter 1" and choose precommand time to be 0.693 times of system time constant. Table 5.6 shows that smaller the system time constant, the better the system performance for separated-mixture system. Similar effect on combined-mixture systems can be found from Table 5.7 that systems with smaller time constant have better overall system performance.

Flow Rates Variation Effect

Sprayer system performance also depends on flow rates variation. Consider a step-up and step-down process with an average pump flow rate at 26.1 gpm for the 12 nozzle case. Table 5.8 shows that the smaller flow rate step variation, the better system performance is.

Summary

Spraying system flow characteristics were studied and computer program for analysis flow characteristic was

developed. Application error of spraying systems caused by system dynamics, nonuniform flow distribution, and transportation delay were discussed and formulated. An optimal selection process for boom hose diameter and precommand time to minimizing the integral absolute-application error for combined-mixture spraying systems was developed. If uniform flow distribution is achievable, the best precommand time for existing separated-mixture spraying system is 0.693 times the system time constant. Separated-mixture system performance can be improved by optimal selection of a boom hose diameter and precommand time. The existing separated-mixture system has the advantage of less application error and the combined-mixture system has the advantage of simple system structure. Optimal design and performance of spraying system depends on actual field data.

Table 5.1 Configuration of Test Case

Distance between nozzles (x)	= 20"
C_d (refer to gpm and psi)	= 0.45853
Step-up desired nozzle flowrate (Q_d)	= 2.9 gpm
Step-down desired nozzle flowrate(QO_d)	= 1.45 gpm
k (of Equation 5.5)	= 0.45
t_{cell}	= 8 sec
Time constant of system (τ)	= 1 sec
Mixture Changing Ratio (MCR)	= 0.5
Header length (l_h)	= 3'
Header diameter (d_h)	= 1"

Table 5.2 Results of 12 Nozzles Test Case (even)

Optimal diameter	= 0.43"
Optimal precomand time	= 0.625 sec
Application error in $2*t_{cell}$ period	= 0.614 gallon

Step-up steady-state properties at nozzles

Nozzle	Flowrate (gpm)	Pressure (psi)	Delay Time (sec)
1	2.81	37.6	0.232
2	2.85	38.7	0.284
3	2.89	39.8	0.348
4	2.93	40.7	0.433
5	2.95	41.5	0.56
6	2.97	41.9	0.814

Step-down steady-state properties at nozzles

Nozzle	Flowrate (gpm)	Pressure (psi)	Delay Time (sec)
1	1.41	9.5	0.465
2	1.43	9.7	0.568
3	1.45	9.9	0.696
4	1.46	10.1	0.867
5	1.47	10.3	1.122
6	1.48	10.4	1.631

Table 5.3 Results of 13 Nozzles Test Case (odd)

Optimal diameter = 0.47"
Optimal precomand time = 0.575 sec
Application error in $2*t_{cell}$ period = 0.7 gallon

Step-up steady-state properties at nozzles

Nozzle	Flowrate (gpm)	Pressure (psi)	Delay Time (sec)
0	3.08	45.3	0.194
1	2.82	37.8	0.245
2	2.85	38.6	0.306
3	2.88	39.4	0.382
4	2.9	40.1	0.482
5	2.92	40.7	0.633
6	2.94	41	0.933

Step-down steady-state properties at nozzles

Nozzle	Flowrate (gpm)	Pressure (psi)	Delay Time (sec)
0	1.55	11.4	0.389
1	1.41	9.5	0.48
2	1.43	9.7	0.612
3	1.44	9.8	0.764
4	1.45	10	0.965
5	1.46	10.1	1.267
6	1.46	10.2	1.869

Table 5.4 Application Errors with Different MCRs

MCR	d (in)	t_c (sec)	error (gallon) in 16 seconds	error %
1	0.37	0.55	0.847	12.2
0.75	0.37	0.55	0.739	10.5
0.5	0.43	0.63	0.847	8.8
0.375	0.33	0.63	0.548	7.9
0.25	0.43	0.55	0.49	7.1
0.125	0.6	0.7	0.465	6.8
0	1.4	0.7	0.431	6.2

Table 5.5 Application Errors with Different Cell Sizes (MCR=0.5)

Cell (m)	t_{cell} (sec)	d (in)	t_c (sec)	error (gallon) in $2t_{cell}$ sec	error %
20	6	0.34	0.5	0.537	15.4
30	6	0.4	0.53	0.581	11.1
40	8	0.43	0.63	0.614	8.8
80	16	0.43	0.68	0.645	4.6
120	24	0.54	0.78	0.709	3.4
200	40	0.59	0.79	0.85	2.4

Table 5.6 Time Constant Effect on Separate-Mixture System

τ (sec)	d (in)	t_c (sec)	error (gallon) in 16 seconds	error %
0.25	1	0.17	0.136	2
0.5	1	0.35	0.234	3.4
0.75	1	0.52	0.333	4.8
1	1	0.69	0.432	6.2
1.25	1	0.87	0.532	7.6
1.5	1	1.04	0.63	9.1
2	1	1.39	0.818	11.8

Table 5.7 Time Constant Effect on Combine-Mixture System (MCR=0.5)

τ (sec)	d (in)	t_c (sec)	error (gallon) in 16 seconds	error %
0.25	0.39	0.4	0.469	6.8
0.5	0.42	0.5	0.476	6.8
0.25	0.43	0.53	0.533	7.7
1	0.43	0.63	0.614	6.8
1.5	0.43	0.63	0.812	11.7
2	0.41	0.65	1.033	14.8
2.5	0.4	0.63	1.249	17.9
3	0.4	0.63	1.448	20.8

Table 5.8 Application Errors with Flow Rate Variations (average total flow rate=26.1 gpm, MCR=0.5)

(Q-Q0) (gpm)	d (in)	t_c (sec)	error (gallon) in 16 seconds	error %
34.8	0.45	0.73	0.936	13.4
26.1	0.42	0.7	0.753	10.8
17.4	0.43	0.63	0.614	8.8
8.7	0.43	0.55	0.453	6.5
4.35	0.42	0.58	0.378	5.4
0	0.43	0.48	0.314	4.5

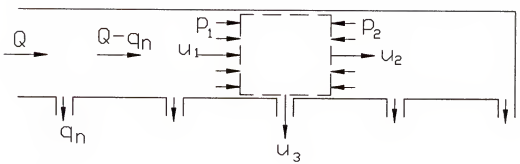

Figure 5.1 Dividing Manifold.

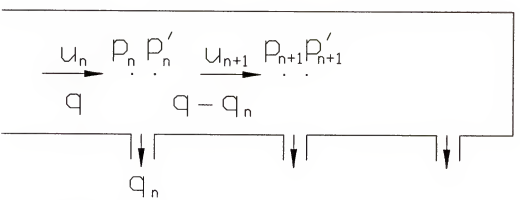

Figure 5.2 Pressure Notations in Nozzle #n.

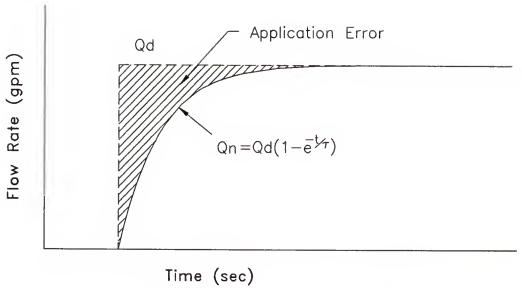

Figure 5.3 Nozzle Flow Step Response and Application Error.

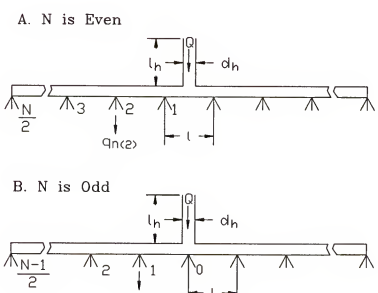

Figure 5.4 Two kinds of Nozzle Arrangements.

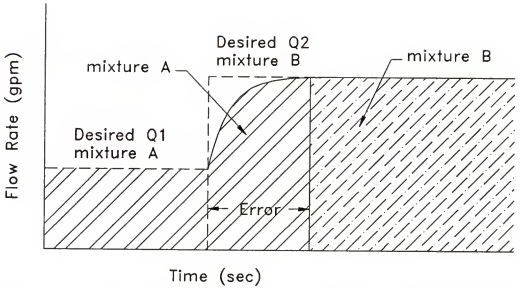

Figure 5.5 Application Error Caused by Transportation Delay.

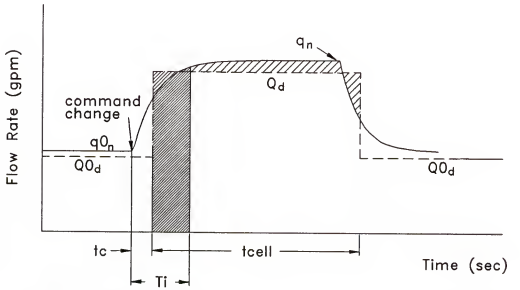

Figure 5.6 Case A Application Error for Step-Up Rate Change (Hatched Area).

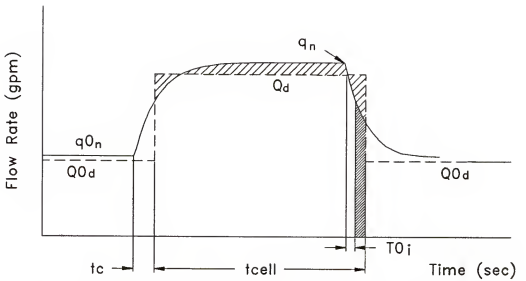

Figure 5.7 Case B Application Error for Step-Up Rate Change (Hatched Area).

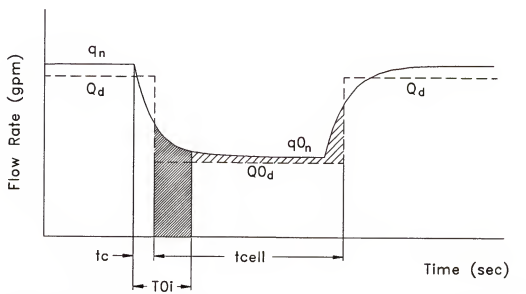

Figure 5.8 Case A Application Error for Step-Down Rate Change (Hatched Area).

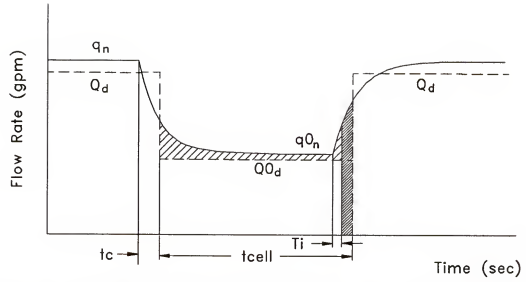

Figure 5.9 Case B Application Error for Step-Down Rate Change (Hatched Area).

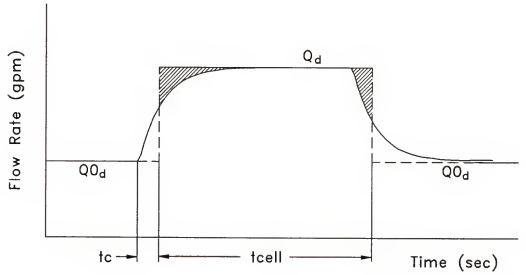

Figure 5.10 Application Error of Separated-Mixture System (Hatched Area).

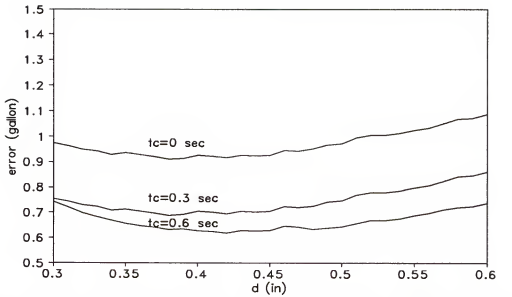

Figure 5.11 Application Error versus Diameter with Constant Precommand Times.

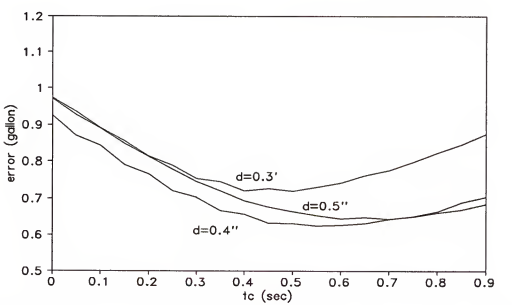

Figure 5.12 Application Error versus Precommand Time with Constant Diameters.

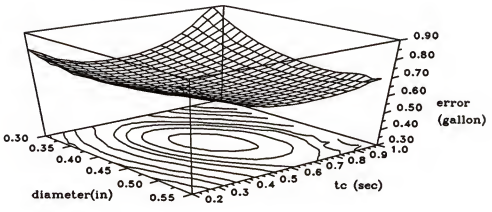

Figure 5.13 Application Error versus Precommand Time (t_c) and Diameter (d).

CHAPTER 6
SIMULATION WITH FIELD DATA

Introduction

Field properties are usually not uniform. For a field with uniform properties, uniform rate application can be performed by utilizing a traditional spraying system with premixed constant concentration mixtures. For fields with nonuniform properties, spatially-variable control can be applied with either separated-mixture spraying systems or combined-mixture spraying systems. It has been shown that optimal selection of boom hose and feedforward precommand time depends on the actual field property variations. In this chapter, simulations of an applicator travelling on paths of the German field with combined-mixture and separated-mixture spraying systems will be performed and the performance of the two systems will be compared.

Pump Flow Rate

Liquid fertilizers are usually diluted and the actual flow rate that pump has to deliver can be expressed by

$$Q_p = \frac{F_r V_a W_a}{37850 \rho C_f}$$

where

Q_p = Desired pump flow rate, gps,

F_r = Fertilizer desired rate, kg/ha,

V_a = Speed of applicator, m/sec,

W_a = Spray width of nozzles, m,

C_f = Concentration of the fertilizer mixture,

ρ = Density of fertilizer mixture, g/cm^3.

For simulation purposes, the following assumptions are made throughout this chapter: the applicator travels at 5 m/sec; both P_2O_5 and K_2O mixtures are of a density equivalent to a specific gravity of 1; the active ingredient concentration of both mixtures is 0.5.

Optimal spraying system design depends on actual field properties. Figures 6.1 and 6.2 display the desired fertilizer application rates for P_2O_5 and K_2O for the German field. The three paths that the applicator travels through are shown in Figure 6.3. Table 6.1 lists the average properties of the desired fertilizer application rates along the three paths. The average total desired application rate (P_2O_5 and K_2O) is 66.2 kg/ha and the standard deviation of total application rate is 41 kg/ha. The high standard deviation of total application rate indicates that the field property is highly nonuniform. The mixture changing ratio (MCR) listed in Table 6.1 is the average MCR from zone to zone along the three paths. These properties will be used for

selecting boom hose diameters and precommand times of both small and large scale spraying systems.

Simulations of Small Scale Spraying Systems

Table 6.2 lists the configurations of a small scale dual-pump combined-mixture system and a separated-mixture spraying system which consists of two identical single pump systems. These configurations are based upon the spraying system modelled in Chapter 3.

Combined-Mixture System

The average total flow rate of the pumps along the three paths is 2.03 gpm for the small scale combined-mixture system to achieve the desired average total application rate of 66.2 kg/ha, and its standard deviation (STD) is 1.26 gpm. The average flow rate for each nozzle is thus 0.406 gpm for this 5 nozzles system. A general guideline for nozzle selection is to select a nozzle that will maintain a nozzle pressure between 20 and 40 psi over all operating conditions (Wolf et al., 1985). A nozzle discharge coefficient (C_d) of 0.074 was chosen to obtain a nozzle pressure of about 30 psi at the average nozzle flow rate. Assuming that the desired total flow rate changes periodically from 3.29 gpm (one STD above the average total flow rate) to 0.77 gpm (one STD below the average total flow rate), the resulting optimal boom hose diameter is 0.18" and precommand time is 0.45 seconds for this small scale combined-mixture spraying system.

Separated-Mixture Systems

The average total pump flow rates along the three paths for a system applying P_2O_5 and a system applying K_2O are 0.878 gpm and 1.152 gpm respectively. To keep nozzle pressure at about 30 psi for the average nozzle flow rate, the nozzle discharge coefficient for system applying P_2O_5 was chosen to be 0.032 and 0.042 for the K_2O system be 0.042. For both of the single pump systems, it is assumed that boom hose diameter is 0.5". The optimal feedforward precommand time is 0.35 seconds for both systems, which is 0.693 times the system time constant 0.5 seconds.

Simulation Results

Simulations for applicator travelling through the three paths of Figure 6.3 were performed. Figures 6.4 to 6.6 display the simulation results of desired and actual fertilizer application rates of P_2O_5 and K_2O along path 1 for nozzle 0 to nozzle 2 of the combined-mixture spraying system. The application rate time histories of nozzle 1 along paths 2 and 3 are shown in Figures 6.7 and 6.8. Figure 6.9 shows the typical results for nozzles of separated-mixture system along path 1. Mixture transportation delay can be seen in Figures 6.3 to 6.8, as the nozzles continue to spray the old mixture until the new mixture arrives at the nozzles. The overall performance along the three paths can be seen in Tables 6.4 and 6.5. For the combined-mixture system, the overall integral absolute error (IAE) is 0.277 gallons, which is 5.4%

of the total desired application rate of 5.139 gallons. The actual volume of the fertilizers applied is 5.11 gallons. For the separated-mixture systems, the IAE is 0.165 gallons, 3.2% of the desired application rate, with 5.105 gallons of actual fertilizers applied.

Simulations of Large Scale Spraying Systems

The configurations of large spraying systems for simulation were listed in Table 6.2. These data are based upon current large applicator designs.

Combined-Mixture System

With the 14 nozzle and 65' long boom hose combined-mixture system, the average total flow rate of the pumps is 20.8 gpm and its standard deviation (STD) is 13 gpm. To keep nozzle pressure at about 30 psi at average nozzle flow rate, the nozzle discharge coefficient (C_d) was selected to be 0.274. The optimal boom hose diameter and precommand time for this combined-mixture system are 0.36" and 0.8 seconds, based on the assumption that the desired total flow rate of the system changes periodically from 33.8 gpm to 7.8 gpm (one STD above and below the average total flow rate).

Separated-Mixture Systems

The average total pump flow rates for the system applying P_2O_5 and the system applying K_2O are 8.98 gpm and 11.8 gpm along the three paths. To maintain a nozzle pressure of about 30 psi at average nozzle flow rate, the nozzle discharge coefficient for the system applying P_2O_5 was chosen to be 0.13

and 0.157 for the K_2O system. Both of the single pump systems were assumed a boom hose diameter of 1" and a feedforward precommand time of 0.7 seconds (about 0.693 times of the system time constant 1 second).

Simulation Results

Figures 6.10 to 6.12 show the fertilizer application rate histories of nozzle 5 of the combined-mixture system along paths 1, 2, and 3. Simulation results of nozzle 5 of the separated-mixture systems along path 1 are shown in Figure 6.13. The overall performance of the combined-mixture system can be seen in Table 6.6. The total desired application rate is 52.759 gallons and actual rate applied is 52.293 gallons. The resulting IAE is 4.949 gallons, 9.4% of the desired rate. Table 6.7 shows the results of separated-mixture systems. Here the IAE is 3.378 gallons, 6.4% of the total desired rate 52.729 gallons. The actual rate applied for the separated-mixture system is 52.157 gallons.

System Performance Comparison

Simulation results along each path were also tabulated in Tables 6.4 to 6.7 for different types of systems. Tables 6.4 and 6.5 list the simulation results of small scale system with and without precommand. It can seen from Table 6.4 that the total desired application rate of P_2O_5 is 1.045 gallons along path 1 for small scale systems. With 0.45 seconds precommand, the small scale combined-mixture system actually applies 1.047 gallons of P_2O_5 and the IAE is 0.042 gallons, which is 4% of

desired rate. Tables 6.6 and 6.7 show the results of large scale system with and without precommand. From the results shown in Tables 6.4 to 6.7, it can be found

(1) Systems perform better with proper precommands (IAE is 5.4% of total desired application rate for small combined-mixture system with precommand and is 7.3% without precommand).

(2) Separated-mixture systems have less error than combined-mixture systems (0.165 gallons for the small separated-mixture system and 0.277 gallons for the small combined-mixture system with precommand).

(3) Small scale systems have better performance than large scale systems (IAE 5.4% of desired total desired application rate for the small combined-mixture system and 9.4% for the large combined-mixture system with precommand).

Simulations of traditional pre-mixed constant concentration sprays were also performed and results are listed in Table 6.8. It is assumed that these systems apply the average desired rates along the three paths. The overall IAE of traditional systems are 57.5% of desired application rates. This shows that the performance of traditional spraying systems is worse than spatially-variable control spraying systems in this particular case studied.

Table 6.1 Desired Fertilizer Rates Properties

P_2O_5 average desired rate	= 28.6 kg/ha
K_2O average desired rate	= 37.6 kg/ha
Average total desired rate	= 66.2 kg/ha
Standard deviation of total desired rate	= 41 kg/ha
Mixture changing ratio	= 0.218
Cell size	= 40 m

Table 6.2 Configurations of Small Spraying Systems

A. Combined-mixture system	
Total nozzles	= 5
Distance between nozzles	= 19"
Header diameter	= 0.5"
Header length	= 3'
τ	= 0.5 sec
V_a	= 5 m/sec
t_{cell}	= 8 sec
Nozzle C_d	= 0.074 (gpm/psi$^{\frac{1}{2}}$)
Boom hose diameter	= 0.18"
Precommand time	= 0.45 sec
B. Separated-mixture systems	
Total nozzles	= 5
Distance between nozzles	= 19"
Header diameter	= 0.5"
Header length	= 3'
τ	= 0.5 sec
V_a	= 5 m/sec
t_{cell}	= 8 sec
Nozzle C_d (P_2O_5 system)	= 0.032 (gpm/psi$^{\frac{1}{2}}$)
Nozzle C_d (K_2O system)	= 0.042 (gpm/psi$^{\frac{1}{2}}$)
Boom hose diameter	= 0.5"
Precommand time	= 0.35 sec

Table 6.3 Configurations of Large Spraying Systems

A. Combined-mixture system

Total nozzles	= 14
Distance between nozzles	= 60"
Header diameter	= 1"
Header length	= 3'
τ	= 1 sec
V_a	= 5 m/sec
t_{cell}	= 8 sec
Nozzle C_d	= 0.27 (gpm/psi$^{1/2}$)
Boom hose diameter	= 0.37"
Precommand time	= 0.8 sec

B. Separated-mixture systems

Total nozzles	= 14
Distance between nozzles	= 60"
Header diameter	= 1"
Header length	= 3'
τ	= 1 sec
V_a	= 5 m/sec
t_{cell}	= 8 sec
Nozzle C_d (P_2O_5 system)	= 0.117 (gpm/psi$^{1/2}$)
Nozzle C_d (K_2O system)	= 0.154 (gpm/psi$^{1/2}$)
Boom hose diameter	= 1"
Precommand time	= 0.7 sec

Table 6.4 Performance of Small Combined-Mixture System

		PATH 1		PATH 2		PATH 3		Total
		P_2O_5	K_2O	P_2O_5	K_2O	P_2O_5	K_2O	
t_c	desired rate(g)	1.045	1.293	0.833	1.114	0.341	0.513	5.139
0.45	actual(g)	1.047	1.275	0.823	1.116	0.327	0.522	5.11
	IAE(g)	0.042	0.065	0.054	0.056	0.024	0.036	0.277
	error %	4	4.4	6.4	5	7.1	6.9	5.4
0	actual(g)	1.043	1.257	0.819	1.113	0.323	0.518	5.073
	IAE(g)	0.055	0.075	0.085	0.088	0.031	0.041	0.375
	error %	5.2	5.8	10.2	7.9	9	8.1	7.3

Table 6.5 Performance of Small Separated-Mixture Systems

		PATH 1		PATH 2		PATH 3		Total
		P_2O_5	K_2O	P_2O_5	K_2O	P_2O_5	K_2O	
t_c	desired rate(g)	1.045	1.293	0.833	1.114	0.341	0.513	5.139
0.35	actual(g)	1.041	1.278	0.828	1.111	0.338	0.509	5.105
	IAE(g)	0.028	0.043	0.037	0.043	0.006	0.014	5.185
	error %	2.1	3.3	4.5	3.3	3.3	2.7	3.2
0	actual(g)	1.038	1.263	0.824	1.109	0.335	0.506	5.075
	IAE(g)	0.032	0.05	0.056	0.062	0.01	0.018	0.228
	error %	3	3.9	6.7	5.5	2.9	3.6	4.4

Table 6.6 Performance of Large Combined-Mixture System

		PATH 1		PATH 2		PATH 3		Total
		P_2O_5	K_2O	P_2O_5	K_2O	P_2O_5	K_2O	
t_c	desired rate(g)	10.727	13.273	8.548	11.439	3.503	5.269	52.759
0.8	actual(g)	10.735	12.982	8.443	11.466	3.323	5.344	52.293
	IAE(g)	0.755	1.148	0.995	1.09	0.372	0.589	4.949
	error %	7	8.6	11.6	9.5	10.6	11.2	9.4
0	actual(g)	10.656	12.609	8.365	11.418	3.249	5.251	51.458
	IAE(g)	0.99	1.438	1.538	1.668	0.463	0.698	6.795
	error %	9.2	10.8	18	14.6	13.2	13.1	12.9

Table 6.7 Performance of Large Separated-Mixture Systems

		PATH 1		PATH 2		PATH 3		Total
		P_2O_5	K_2O	P_2O_5	K_2O	P_2O_5	K_2O	
t_c	desired rate(g)	10.727	13.273	8.548	11.439	3.503	5.269	52.759
0.7	actual(g)	10.663	12.972	8.485	11.4	3.443	5.194	52.157
	IAE(g)	0.453	0.871	0.763	0.87	0.133	0.288	3.378
	error %	4.2	8.9	8.9	7.6	3.8	5.5	6.4
0	actual(g)	10.598	13.273	8.421	11.36	3.382	5.117	52.151
	IAE(g)	0.676	1.084	1.168	1.313	0.203	0.386	4.83
	error %	6.3	8.2	13.7	11.47	5.8	7.3	9.2

Table 6.8 Performance of Traditional Systems

		PATH 1		PATH 2		PATH 3		Total
		P_2O_5	K_2O	P_2O_5	K_2O	P_2O_5	K_2O	
Small System	desired rate(g)	1.045	1.293	0.833	1.114	0.341	0.513	5.139
	actual(g)	0.817	1.076	0.7	0.922	0.7	0.922	5.139
	IAE(g)	0.258	0.757	0.401	0.669	0.377	0.493	2.955
	error %	24.7	58.5	48.2	60	110.6	48.2	57.5
Large System	desired rate(g)	10.727	13.273	8.548	11.439	3.503	5.269	52.759
	actual(g)	8.392	11.045	7.193	9.467	7.193	9.467	52.759
	IAE(g)	2.65	7.766	4.119	6.862	3.873	5.068	30.3
	error %	24.7	58.5	48.2	60	110.6	96.2	57.5

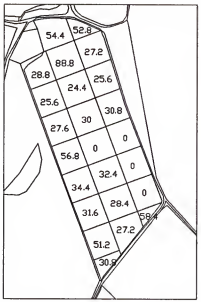

Figure 6.1 Desired Fertilizer P_2O_5 Application Rates (kg/ha).

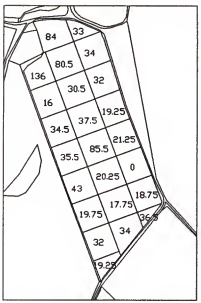

Figure 6.2 Desired Fertilizer K_2O Application Rates (kg/ha).

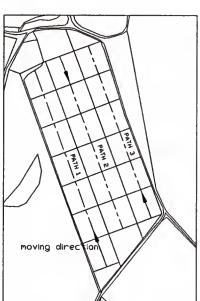

Figure 6.3 Paths of German Field.

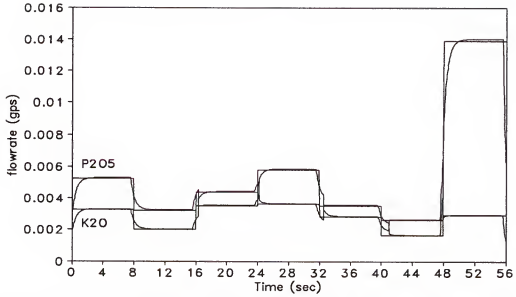

Figure 6.4 Small Combined-Mixture System Nozzle 0 Simulation along Path 1.

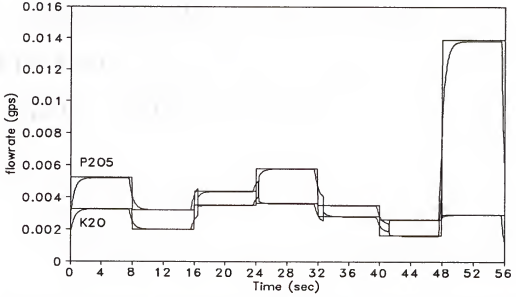

Figure 6.5 Small Combined-Mixture System Nozzle 1 Simulation along Path 1.

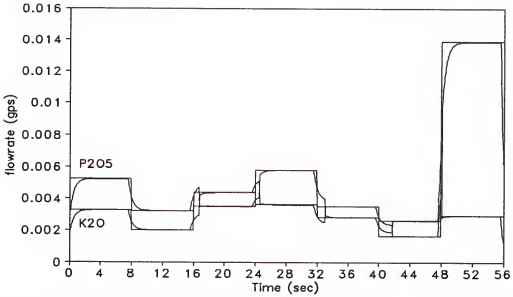

Figure 6.6 Small Combined-Mixture System Nozzle 2 Simulation along Path 1.

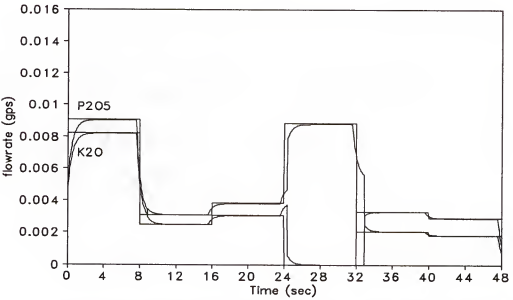

Figure 6.7 Small Combined-Mixture System Nozzle 1 Simulation along Path 2.

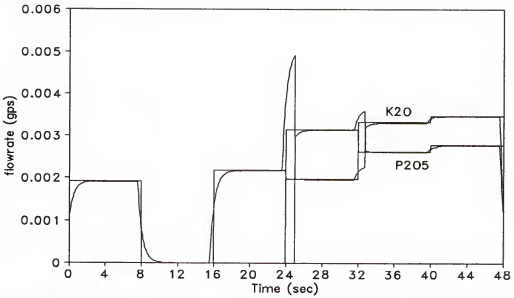

Figure 6.8 Small Combined-Mixture System Nozzle 1 Simulation along Path 3.

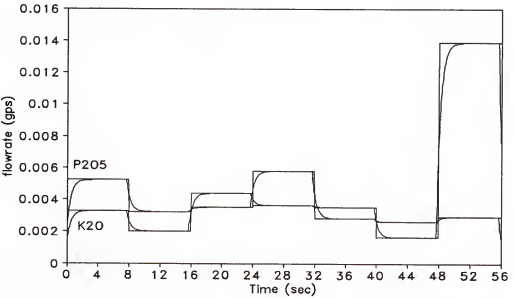

Figure 6.9 Small Separated-Mixture Systems Nozzle 1's Simulation along Path 1.

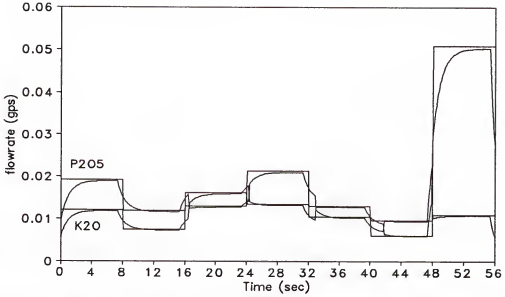

Figure 6.10 Large Combined-Mixture System Nozzle 5 Simulation along Path 1.

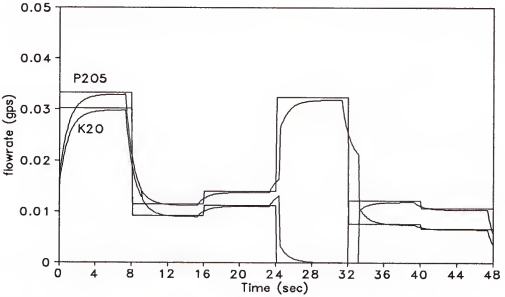

Figure 6.11 Large Combined-Mixture System Nozzle 5 Simulation along Path 2.

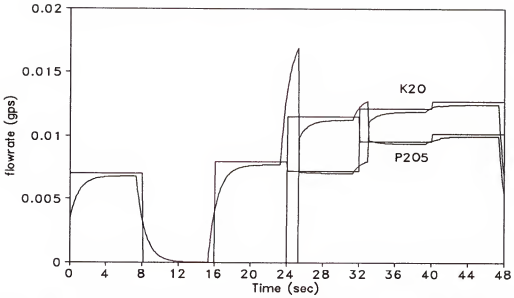

Figure 6.12 Large Combined-Mixture System Nozzle 5 Simulation along Path 3.

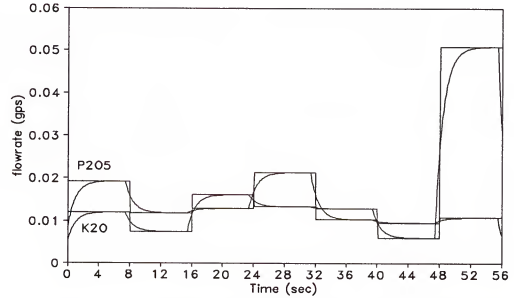

Figure 6.13 Large Separated-Mixture System Nozzle 5's Simulation along Path 1.

CHAPTER 7
CONCLUSIONS AND RECOMMENDATIONS

Conclusions

This research developed techniques to aid spatially-variable control of liquid fertilizer and pesticide application in three major aspects: spatial data handling, pump flowrate control, and optimal design of spraying systems.

A spatial data handling system using a Geo/SQL GIS was developed. Field data from Germany were used to build up the system. This system can determine fertilizer application based on field data. It shows that a commercial GIS can be applied for spatially-variable control purposes.

A state-space model of a selected liquid spraying system was derived. Optimal computer pump flow control was conducted using Linear Quadratic Gaussian (LQG) control theory, which combines a Linear Quadratic Regulator (LQR) and a Kalman filter. Multiple pumps' flowrates estimation using a pressure transducer through the Kalman filter was implemented without flowmeters. LQG closed-loop spraying system control improved both transient and steady-state flowrate response. This multiple-input/multiple-output (MIMO) control scheme is suitable for spatially-variable liquid combined-mixture spraying systems, since such spraying systems are essentially MIMO.

Tools for analysis and design of liquid spraying systems were developed. The flow characteristics along a boom hose has been studied as a divided flow manifold problem. Application error caused by system transient response, nonuniform flow distribution, and transportation delay was formulated. The optimization of boom hose diameters and feedforward precommand times was performed by minimizing the integral absolute application error, which illustrated a methodology for overall spraying system optimization. Design examples were demonstrated to show the utility of this concept. Programs for flow characteristic and optimal boom hose diameter and precommand time selection were developed and can be used as spraying system design tools.

Because of mixture transportation delay, combined-mixture systems have higher application error than existing commercial separated-mixture systems. However, combined-mixture systems have simpler system structures resulting in lower weights and costs. With the optimal control and design techniques developed in this research, the performance of spatially-variable spraying systems can be improved and the goals of spatially-variable control, environmental protection and more economic use of fertilizers and pesticides, can be achieved.

Recommendations

Design Recommendation

Based on the findings in this study, some general guidelines on spatially-variable control liquid spraying

systems design are given below:

(1) Spraying systems with shorter system response time tend to have less application errors. To have a shorter system response time, the boom hose should have higher bulk modulus and the total system volume should be as small as possible.

(2) For combined-mixture systems, header hose length and diameter should be as small as possible to reduce application error caused by transportation delay.

(3) Proper precommand can improve system performance. For separated-mixture systems with uniform flow distribution, the optimal precommand time is 0.693 times the system time constant. For combined-mixture systems, optimal precommand times and boom hose diameters can be selected using techniques developed in this study.

Future Research Recommendation

The overall error in spatially-variable control of liquid fertilizer/pesticide application includes application errors of applicators, inaccuracies of mobile locators, and the quantization of GIS data. Minimizing applicator application error due to the transient, transportation delay, and nonuniform flow distribution has been studied in this research. Further study on modelling and minimizing locator's error and GIS error should be done to improve spatially-variable control of liquid fertilizer/pesticide overall performance.

While this research has analyzed spatially-variable control of a liquid fertilizer/pesticide applicator on a small scale dual-pump spraying system, further research could concentrate on modelling spraying systems with large pumps and building a large-sized multiple pumps combined-mixture system integrated with GPS for a field test.

APPENDIX A
PROGRAM FERTILIZER.C

```
/* This program will update fertilizer required rates from the
   predicted yield and soil data                                */

#include <stdio.h>
#include <ctype.h>

EXEC SQL BEGIN DECLARE SECTION;
VARCHAR uid[20];
VARCHAR pwd[20];
float s_p2o5,s_k2o,pre_yield,f_k2o;
float f_p2o5;
char soil_type[3];
int i;
EXEC SQL END DECLARE SECTION;
EXEC SQL INCLUDE SQLCA;
main()
{
   strcpy(uid.arr,"CONTROLAB");
   uid.len=strlen(uid.arr);
   strcpy(pwd.arr,"WANG");
   pwd.len=strlen(pwd.arr);

   EXEC SQL WHEREVER SQLERROR GOTO errexit;
   EXEC SQL CONNECT :uid IDENTIFIED BY :pwd;
   for(i=1;i<25;i++)
   {
      EXEC SQL SELECT  SOIL_TYPE,S_P2O5,S_K2O,PRE_YIELD
      INTO :soil_type,:s_p2o5,:s_k2o,:pre_yield
      FROM ZONE
      WHERE ZONE#=:i;

/* calculating fertilizer P2O5 & K2O desired rate according to
   Tables 2.2 & 2.3                                             */
      if(s_p2o5 < 8.0)
         f_p2o5=8.0*pre_yield+90.0;
      if( 8.0 <= s_p2o5 && s_p2o5< 15.0)
         f_p2o5=8.0*pre_yield+40.0;
      if( 15.0 <= s_p2o5 && s_p2o5 < 25.0)
         f_p2o5=8.0*pre_yield;
      if( 25.0 <= s_p2o5 && s_p2o5 <= 40.0)
         f_p2o5=4.0*pre_yield;
      if(s_p2o5 > 40.0)
         f_p2o5=0.0;
```

```
/* Tu is heavy soil and all others are medium soil */
      if ( soil_type[0] == 'T' && soil_type[1]== 'u' )
      {
         if( s_k2o < 10.0)
            f_k2o=5.0*pre_yield+100.0;
         if( 10.0 <= s_k2o && s_k2o < 20.0 )
            f_k2o=5.0*pre_yield+50.0;
         if( 20.0 <= s_k2o && s_k2o < 35.0 )
            f_k2o=5.0*pre_yield;
         if( 35.0 <= s_k2o && s_k2o <= 50.0 )
            f_k2o=2.50*pre_yield;
         if( s_k2o > 50.0 )
            f_k2o=0.0;
      }
      else
     {
         if( s_k2o < 8.0 )
            f_k2o=5.0*pre_yield+100.0;
         if( 8.0 <= s_k2o && s_k2o < 15.0 )
            f_k2o=5.0*pre_yield+50.0;
         if( 15.0 <= s_k2o && s_k2o < 30.0 )
            f_k2o=5.0*pre_yield;
         if( 30.0 <= s_k2o && s_k2o < 45.0 )
            f_k2o=2.50*pre_yield;
         if( s_k2o >= 45.0 )
            f_k2o=0.0;
      }

      EXEC SQL UPDATE ZONE
      SET F_P2O5=:f_p2o5,F_K2O=:f_k2o
      WHERE ZONE#=:i;
      EXEC SQL COMMIT WORK;
   }
   EXEC SQL COMMIT WORK RELEASE;
}
```

APPENDIX B
PROGRAM DP.C

```
/* For controlling 5 d3 nozzle tips case */
/* nominal model obtained at( 0.008, 0.0075, 25.855) */
#include <dos.h>
#include <stdio.h>
#include <stdlib.h>
#include <conio.h>
#include <math.h>
#include <process.h>
/* Data aquisition board address */
#define BASE_ADDRESS      0x2ec
#define COMMAND_REGISTER 0x2ed
#define STATUS_REGISTER   0x2ed
#define DATA_REGISTER     0x2ec
#define COMMAND_WAIT      0x4
#define WRITE_WAIT        0x2
#define READ_WAIT         0x5
#define CSTOP             0xf
#define CCLEAR            0x1
#define CADIN             0xc
#define CDAOUT            0x8
#define CERROR            0x2
#define FACTOR            4096
#define RANGE             20
#define OFFSET            10

void initial( void );
void write_da( int, float );
float read_ad( int);
void _dos_gettime(struct dostime_t *time);
void volt_in( float, float, float);

int k;
float   ess1[3], ess2[3], ess3[3];
float Cd=0.043,
/* System mosel x(k+1)=Ax(k)+Bu(k)  */
/* Matrix A  */
      a11=0.1453,       a12=-0.013302,     a13=-1.3068e-4,
      a21=-0.0079254,   a22=0.23997,       a23=-1.0462e-4,
      a31=85.643,       a32=102.12,        a33= 0.89163,
/* Matrix B  */
      b11=0.0014971,    b12=-1.4589e-5,    b13=1.8392e-4,
      b21=-1.2508e-5,   b22=1.1222e-3,     b23=1.1899e-4,
      b31=0.19087,      b32=0.13488,       b33=-1.5335,
```

```
/*Inv(B)    */
      ib11=657.92,    ib12=-0.92221,    ib13=0.078836,
      ib21=-1.3379,   ib22=882.87,      ib23=0.068349,
      ib31=81.1773,   ib32=77.541,      ib33=-0.63629,
/* LQR gain K */
      k11=86.9,        k12=18.85,        k13=0.173,
      k21=17.73,       k22=147.66,       k23=0.204,
/* Kalman gain L */
      l11=0.005593,    l21=0.0004377,    l31=0.93563;

main()
{
   float tt,d;
   float x_b1[451] , x_b2[451] , x_b3[451];
   float x_h1[451] , x_h2[451] , x_h3[451];
   float q1[3], q2[3], qb, po[3],u1[451],u2[451];
   float x_mea3[451] ,x_mea1[451], x_mea2[451], x_error3;
   int id=0, tp=0, i, j;
   unsigned char tihs, tis, ts, ths;
   struct dostime_t t, t1;
   FILE    *flow;
   float  a1temp, a2temp, detb;
   float  Kpv1=0.0622, Kvn1=3.0201, Knq1=5.96e-4, C11=5.8e-5,
          Kvq1, Kpq1;
   float  Kpv2=0.09024, Kvn2=4.3029, Knq2=3.5e-4, C12=1.41e-5,
          Kvq2, Kpq2;

   initial();
   flow=fopen("d3_5.dat","w");
   Kvq1=Kvn1*Knq1;  Kpq1=Kpv1*Kvn1*Knq1;
   Kvq2=Kvn2*Knq2;  Kpq2=Kpv2*Kvn2*Knq2;
   q1[0]=1.0;  q1[1]=1.0;  q1[2]=1.0;
   q2[0]=1.0;  q2[1]=1.0;  q2[2]=1.0;

   for(k=0;k<3;k++)
   {
      while( q1[k] >= 0.0133 )
      {
         printf( "Input step 1 desire q1[%d]= ",k );
         scanf( "%f", &q1[k] );
      }
      while( q2[k] >= 0.0133 )
      {
         printf( "Input step 1 desire  q2[%d]= ",k );
         scanf( "%f", &q2[k] );
      }
      qb=q1[k]+q2[k];
      po[k]=144.0*qb*qb/Cd/Cd;
      volt_in(q1[k],q2[k],po[k]);
   }

   x_h1[0] = 0.0;  x_h2[0] = 0.0;  x_h3[0]=0;
```

```
   u1[0] = 0.0;    u2[0] = 0.0;
   d=ess3[0];
   _dos_gettime(&t);
   tihs=t.hsecond;
   for( id=1 ; id<433 ; id++ )
   {
/* Time update  */
/* predict x[i] from u[i-1] and estimated x[i-1] */
      x_b1[id]=a11*x_h1[id-1]+a12*x_h2[id-1]+a13*x_h3[id-1]
               +b11*u1[id-1]+b12*u2[id-1]+b13*d;
      x_b2[id]=a21*x_h1[id-1]+a22*x_h2[id-1]+a23*x_h3[id-1]
               +b21*u1[id-1]+b22*u2[id-1]+b23*d;
      x_b3[id]=a31*x_h1[id-1]+a32*x_h2[id-1]+a33*x_h3[id-1]
               +b31*u1[id-1]+b32*u2[id-1]+b33*d;
      if( x_b1[id] < 0.0 ) x_b1[id] = 0.0;
      if( x_b2[id] < 0.0 ) x_b2[id] = 0.0;
      if( x_b3[id] < 0.0 ) x_b3[id] = 0.0;

 /* measure pressure, 20.0 is the psi/volt factor and 1.0 is
    the offset of the pressure sensor   */
      x_mea3[id] = read_ad(0)*20.0-1.0;
      if( x_mea3[id] < 0.0 ) x_mea3[id] = 0.0;
      x_mea1[id]= u1[id-1]*Kvq1-x_mea3[id]*(Cl1+Kpq1);
      x_mea2[id]= u2[id-1]*Kvq2-x_mea3[id]*(Cl2+Kpq2);
      if( x_mea1[id] < 0.0 ) x_mea1[id] = 0.0;
      if( x_mea2[id] < 0.0 ) x_mea2[id] = 0.0;

 /* Measurement update     */
      x_error3=x_mea3[id]-x_b3[id];
      x_h1[id]=x_b1[id]+l11*x_error3;
      x_h2[id]=x_b2[id]+l21*x_error3;
      x_h3[id]=x_b3[id]+l31*x_error3;
      if( x_h1[id] < 0.0 ) x_h1[id] = 0.0;
      if( x_h2[id] < 0.0 ) x_h2[id] = 0.0;
      if( x_h3[id] < 0.0 ) x_h3[id] = 0.0;

 /* Update linearized model using new from measurement updated
    states                                                    */

      if(id<145)
      {
         u1[id]=ess1[0]-k11*(x_h1[id]-q1[0])
                -k12*(x_h2[id]-q2[0])-k13*(x_h3[id]-po[0]);
         u2[id]=ess2[0]-k21*(x_h1[id]-q1[0])
                -k22*(x_h2[id]-q2[0])-k23*(x_h3[id]-po[0]);
      }

      if(id>=145 && id <289)
      {
         u1[id]=ess1[1]-k11*(x_h1[id]-q1[1])
                -k12*(x_h2[id]-q2[1])-k13*(x_h3[id]-po[1]);
         u2[id]=ess2[1]-k21*(x_h1[id]-q1[1])
```

```
                -k22*(x_h2[id]-q2[1])-k23*(x_h3[id]-po[1]);
        d=ess3[1];
    }

    if(id>=289 )
    {
        u1[id]=ess1[2]-k11*(x_h1[id]-q1[2])
                -k12*(x_h2[id]-q2[2])-k13*(x_h3[id]-po[2]);
        u2[id]=ess2[2]-k21*(x_h1[id]-q1[2])
                -k22*(x_h2[id]-q2[2])-k23*(x_h3[id]-po[2]);
        d=ess3[2];
    }
/* Check saturation  */
    if(u1[id] >= 10.0) u1[id]=10.0;
    if(u1[id] <=  0.0) u1[id]=0.0;
    if(u2[id] >= 10.0) u2[id]=10.0;
    if(u2[id] <= 0.0 ) u2[id]=0.0;
/* Output Commands */
    write_da( 0, u1[id]/2.0 );
    write_da( 1, u2[id]);
    printf("%f %f %f\n",x_b3[id],x_b1[id],x_b2[id]);

    while( tp < 5 )
    {
        _dos_gettime(&t1);
        tp=abs((int)t1.hsecond-(int)tihs);
    }
    tihs=t1.hsecond;
    tp=0;
}
/* Reset data acquisition  board */
write_da(1,0.0); write_da(0,0.0);
outp(COMMAND_REGISTER, 0xf);

for(j=0;j<433;j++)
{
    fprintf(flow,"%f %f %f %f %f %f %f %f\n " ,u1[j],u2[j],
     x_mea1[j],x_mea2[j],x_mea3[j],x_h1[j],x_h2[j],x_h3[j]);
}
fclose(flow);
}
```

```
void write_da( int channel, float value )
{
   int data_value, status, low, high;
   data_value=(int)( (value+OFFSET)*FACTOR/RANGE );
   if( data_value > (FACTOR - 1) )
      data_value=FACTOR - 1;
   high=(int)(data_value/256);
   low=data_value-high*256;
   while( ( inp( STATUS_REGISTER ) & 0x06 ) != COMMAND_WAIT );
      outp( COMMAND_REGISTER, CDAOUT );

   while( inp( STATUS_REGISTER ) & WRITE_WAIT );
      outp ( DATA_REGISTER, channel );

   while (inp( STATUS_REGISTER ) & WRITE_WAIT );
      outp( DATA_REGISTER, low );

   while (inp( STATUS_REGISTER ) & WRITE_WAIT );
      outp( DATA_REGISTER, high );

   while( (inp(STATUS_REGISTER)& 0x06) != COMMAND_WAIT);
      status=inp( STATUS_REGISTER );
   if ( status & 0x80 )
   {
      printf("Write error!!\n");
   }
}

void initial( void )
{
   outp( COMMAND_REGISTER, CSTOP );
   inp( DATA_REGISTER );
   while( (inp( STATUS_REGISTER ) & 0x06) != COMMAND_WAIT );
     outp( COMMAND_REGISTER, CCLEAR );
   write_da( 0, 0.0 );
   write_da( 1, 0.0 );
}
```

```
float read_ad( int channel)
{
   int data_value, high, low, status, gain_code = 0;
   float result;

   while( (inp( STATUS_REGISTER ) & 0x06 ) != COMMAND_WAIT );
      outp( COMMAND_REGISTER, CADIN );

   while( inp( STATUS_REGISTER ) & WRITE_WAIT );
      outp( DATA_REGISTER, gain_code );

   while( inp( STATUS_REGISTER ) & WRITE_WAIT );
      outp( DATA_REGISTER, channel );

   while (!(inp( STATUS_REGISTER ) & READ_WAIT) );
      low=inp( DATA_REGISTER );

   while (!(inp( STATUS_REGISTER ) & READ_WAIT) );
      high=inp( DATA_REGISTER );

   data_value=high*256 + low;

   result=20.0*data_value/4096.0-10.0;

   while( inp( STATUS_REGISTER ) & 0x06 != COMMAND_WAIT );
      status=inp( STATUS_REGISTER );
   if( status & 0x80 )
      printf("Read error...\n");

     return result;
}


void volt_in(float qq1, float qq2, float ppo)
{
   float  s1, s2,s3 ,detb;
   s1=(1.0-a11)*qq1-a12*qq2-a13*ppo;
   s2=(-a21)*qq1+(1.0-a22)*qq2-a23*ppo;
   s3=(-a31)*qq1-a32*qq2+(1.0-a33)*ppo;
   ess1[k]=ib11*s1+ib12*s2+ib13*s3;
   ess2[k]=ib21*s1+ib22*s2+ib23*s3;
   ess3[k]=ib31*s1+ib32*s2+ib33*s3;
}
```

APPENDIX C
PROGRAM POWELL.C

```
#include <math.h>
#include <stdio.h>
#include <dos.h>
#include <float.h>
#include <stdlib.h>

int NZ, N, EVEN, NEGATIVE, UP=1, DOWN=1;
float p[15], pa[15], pz[15], q[15], qn[15], qn0[15], delt[15],
      delt0[15], vel[15], Q, Q0, x, Qd, Qd0, t_cell, tc, dh,
      lh, th, MCR, tau, d ,d_l=0.125/12.0, d_u=1.5/12.0,
      t_l=0.0, t_u=10.0, t_i, d_i, Cd, Kl=0.45, s1, s2,
      Kscal=448.0, F2G=7.4667, Va, Cell, Cdg;
float errfun(void);
void golden(void);
void flow(void);

main ()
{
   int i,ii=0,Ione, mm, flag1, flag2=0, flag3=0;
   float derr, ERR_opt, DL, DH, SL, S[3][3], tt=0.0 ,tt1, tt2,
         dell, d1, t1, S_ran, tttt, dlow, dhigh, tlow, thigh,
         tc_opt, d_opt;
/* Input sprayer system configuration */
   printf("Input sprayer system configuration:\n");
   printf("NZ= ");
   scanf("%d",&NZ);
   printf("Va= m/sec ");
   scanf("%f",&Va);
   printf("Cell size (m)=");
   scanf("%f ",&Cell);
   printf("Time constant tau(sec)= ");
   scanf("%f",&tau);
   printf("Kl= ");
   scanf("%f",&Kl);
   printf("Distance between nozzles=(in)");
   scanf("%f",&x);
   printf("header hose diameter dh(in)= ");
   scanf("%f",&dh);
   printf("header hose length lh(ft)= ");
   scanf("%f",&lh);
   printf("High Flow Rate Q(gpm)= ");
   scanf("%f",&Q);
   printf("Low Flow Rate Q0(gpm)= ");
   scanf("%f",&Q0);
```

```
   printf("MCR= ");
   scanf("%f",&MCR);
   printf("Cd=?");
   scanf("%f",&Cdg);
   Cd=Cdg/Kscal;
   t_cell=Cell/Va;
   dh=dh/12.0;
   x=x/12.0;
   EVEN=1;
   N=floor(NZ/2.0);
   if((NZ/2.0) != N)
   {
      EVEN=0;;
   }
/* check the low bound of diameter d which has feasible
solution */
   DL=d_l; DH=d_u; d=DL; d_i=DL;
   flow();
   if(NEGATIVE)
   {
      do
      {
         d=(DL+DH)/2.0;
         flow();
         if(NEGATIVE )
            DL=d;
         if(!NEGATIVE )
            DH=d;
         ii=ii+1;
      }while(ii<=20);
      d_i=d_l=DH;
   }

 /* Using powell method to find the optimal d and tc */
   derr=1.0;ERR_opt=1.0;
   S[0][0]=1.0;S[1][0]=0.0;
   S[0][1]=0.0;S[1][1]=1.0;
   d=d_i;tc=t_i=0.0; dell=0.1;
   Ione=0;
   do
   {
      Ione=Ione+1;
      d1=d_i; t1=t_i;
      for(mm=0;mm<2;mm++)
      {
         s1=S[0][mm]; s2=S[1][mm];
         SL=sqrt(s1*s1+s2*s2);
         if(d_i != d_l )
         {
            d=d_i+dell*s1/SL; tc=t_i+dell*s2/SL;
            tt1=errfun();
            d=d_i-dell*s1/SL; tc=t_i-dell*s2/SL;
```

```
            tt2=errfun();
            if(tt1>tt && tt2<tt)
            {
               s1=-s1;s2=-s2;
            }
            if(tt1>=tt && tt2>=tt)
            {
              flag2=1;
              s1=0.0;s2=0.0;
            }
          }
          golden();
          d_i=d;t_i=tc;
          tt=errfun();
       }
       s1=S[0][2]=d_i-d1; s2=S[1][2]=t_i-t1;
       if(s1!=0.0 && s2!=0.0)
       {
          SL=sqrt(s1*s1+s2*s2);
          d=d_i+dell*S[0][2]/SL; tc=t_i+dell*S[1][2]/SL;
          tt1=errfun();
          d=d_i-dell*S[0][2]/SL; tc=t_i-dell*S[1][2]/SL;
          tt2=errfun();
       }
       flag1=0;
       if(tt<=tt1 && tt<=tt2)
       {
          flag1=1;
       }
       if(flag1==0 && flag2==0)
       {
          if(tt1>tt && tt2<tt )
          {
             s1=-s1;s2=-s2;
             S[0][2]=s1;S[1][2]=s2;
          }
          golden();
          d_i=d;t_i=tc;
          tt=errfun();
/* update new searching directions */
          for(mm=0;mm<2;mm++)
          {
             S[0][mm]=S[0][mm+1]; S[1][mm]=S[1][mm+1];
          }
       }
       if(flag1==1 || flag2==1)
       {
          flag1=0;
          flag2=0;
          flag3=1;
       }
       derr=fabs((double)(ERR_opt-tt));
```

```
      printf("new point: d_i=%f t_i=%f \n",d_i*12.0, t_i);
      ERR_opt=tt;
   }while( Ione<10 && derr>=1e-5 && flag3==0);

    /* using exhausting search to check global minimum */
   dlow=d_i-.025/12.0;
   if(dlow < d_l)
      dlow=d_l;
   dhigh=d_i+.075/12.0;
   tlow=t_i-.15;
   if(tlow<0)
      tlow=0;
   thigh=t_i+.15;
   d=dlow;
   do
   {
      tc=tlow;
      do
      {
         tttt=errfun();
         if(tttt<=ERR_opt)
         {
            d_opt=d;
            tc_opt=tc;
            ERR_opt=tttt;
         }
         tc=tc+0.025;
      }while(tc<thigh);
      d=d+.005/12.0;
   }while(d<dhigh);

   printf("Optimal d=%fin Precomand time=%f sec ERROR=%f
           gallon\n ", d_opt*12.0, tc_opt, ERR_opt);
   d=d_opt; tc=tc_opt;
   flow();
   for(i=EVEN;i<N+1;i++)
   printf("qn[%d]=%f gpm p=%f psi delt[%d]= %f sec \n ",
           i, qn[i]*Kscal, pz[i], i, delt[i]);
}
```

```
/* Subroutine Golden Section Method for one dimension search
*/
void golden(void){

   int NN=200, m;
   float X1, X2, XL, XU, F1, F2, derr1;
   float alfa_d, alfa_t, alfa, au, g;

  /* check bound of search direction */
   if(s1>=0 && s2>=0)
   {
      if(s1>0 && s2>0)
      {
         alfa_d=(d_u-d_i)/s1;
         alfa_t=(t_u-t_i)/s2;
         alfa=min(alfa_d,alfa_t);
      }
      if(s1==0 && s2!=0)
      {
         alfa=(t_u-t_i)/s2;
      }
      if(s1!=0 && s2==0)
      {
         alfa=(d_u-t_i)/s1;
      }
      if(s1==0 && s2==0)
      {
         m=NN;
         au=0.0;
      }
   }
   if(s1<=0 && s2<=0)
   {
      if(s1<0 && s2<0)
      {
         alfa_d=(d_l-d_i)/s1;
         alfa_t=(t_l-t_i)/s2;
         alfa=min(alfa_d,alfa_t);
      }
      if(s1==0 && s2!=0)
      {
         alfa=(t_l-t_i)/s2;
      }
      if(s1!=0 && s2==0)
      {
         alfa=(d_l-d_i)/s1;
      }
      if(s1==0 && s2==0)
      {
         m=NN;
      }
   }
```

```
    if(s1>0 && s2<0)
    {
       alfa_d=(d_u-d_i)/s1;
       alfa_t=(t_l-t_i)/s2;
       alfa=min(alfa_d,alfa_t);
    }
    if(s1<0 && s2>0)
    {
       alfa_d=(d_l-d_i)/s1;
       alfa_t=(t_u-t_i)/s2;
       alfa=min(alfa_d,alfa_t);
    }
    au=alfa;
    d=d_i; tc=t_i;
    g=0.381966;
    d=d_i+alfa*s1; tc=t_i+alfa*s2;
    /* Initial XL and XU */
    XL=0.0;XU=au;
/* Begin golden section one dimension search */
    X1=(1.0-g)*XL+g*XU;
    d=d_i+X1*s1; tc=t_i+X1*s2;
    F1=errfun();
    X2=g*XL+(1.0-g)*XU;
    d=d_i+X2*s1; tc=t_i+X2*s2;
    F2=errfun();
    m=3;
    do
    {
       m=m+1;
       if(F1>F2)
       {
          XL=X1;
          X1=X2;
          F1=F2;
          X2=g*XL+(1.0-g)*XU;
          d=d_i+X2*s1; tc=t_i+X2*s2;
          F2=errfun();
       }
       if(F1<=F2)
       {
          XU=X2;
          X2=X1;
          F2=F1;
          X1=(1.0-g)*XL+g*XU;
          d=d_i+X1*s1; tc=t_i+X1*s2;
          F1=errfun();
          }
          derr1=fabs(F1-F2);
      }while(m<=NN && derr1>=1e-5);

}
```

```
/* Application Error Function */

float errfun()
{
   float t=0;
   int ii,i;
   float ERR,ERR_t1[15],ERR_t2[15];
   float qq1,qq2,q1_a,q2_a,q_cell,q_cell0,Q1;

   Q1=Q;
   for (ii=EVEN;ii<(N+1);ii++)
   {
      qn0[ii]=0;
      delt0[ii]=t_cell;
   }
   if(Q0 !=0)
   {
      Q=Q0;
      flow();
      for (ii=EVEN;ii<(N+1);ii++)
      {
         qn0[ii]=qn[ii];
         delt0[ii]=delt[ii];
      }
   }
   Q=Q1;
   flow();
   for (ii=0;ii<(N+1);ii++)
   {
      ERR_t1[ii]=0;ERR_t2[ii]=0;
   }
   t=tc;
/* get steady-state qn[0],qn[1],qn[2], delt[0],delt[1],delt[2]
*/
   do
   {
      for(ii=EVEN;ii<(N+1);ii++)
      {
     /* calculate qq1 , qq2 */
         q_cell=qn[ii]+(qn0[ii]-qn[ii])*exp(-t_cell/tau);
         q_cell0=qn0[ii]+(q_cell-qn0[ii])*exp(-t_cell/tau);
         if(t<=t_cell)
         {
            qq1=qn[ii]+(qn0[ii]-qn[ii])*exp(-t/tau);
            qq2=qn0[ii]+(q_cell-qn0[ii])*exp(-t/tau);
         }
         if(t> t_cell)
         {
            qq1=qn[ii]+(q_cell0-qn[ii])*exp(-(t-t_cell)/tau);
            qq2=qn0[ii]+(q_cell-qn0[ii])*exp(-(t-t_cell)/tau);
         }
```

```
        if(UP==1)
        {
      /* STEP UP----case delt[ii] >=tc */
         if(delt[ii]>=tc)
         {
          if(t<=delt[ii])
          {
            ERR_t2[ii]=ERR_t2[ii]+qq1*MCR;
       ERR_t1[ii]=ERR_t1[ii]+fabs((double)(Qd-qq1*(1.0-MCR)));
          }
          if(t> delt[ii] && t<=t_cell)
          {
           ERR_t1[ii]=ERR_t1[ii]+fabs((double)(Qd-qq1));
          }
          if(t>t_cell)
          {
            ERR_t1[ii]=ERR_t1[ii]+fabs((double)(Qd-qq2));
          }
         }
/* STEP UP-----case delt[ii]< tc  */
        if(delt[ii] < tc)
        {
         if( t<=t_cell)
         {
          ERR_t1[ii]=ERR_t1[ii]+fabs((double)(Qd-qq1));
         }
         if( t>t_cell && t<= (t_cell+delt0[ii]) )
         {
          ERR_t1[ii]=ERR_t1[ii]+fabs((double)(Qd-qq2));
         }
         if( t> (t_cell+delt0[ii]) )
         {
          ERR_t2[ii]=ERR_t2[ii]+qq2*MCR;
       ERR_t1[ii]=ERR_t1[ii]+fabs((double)(Qd-qq2*(1.0-MCR)));
         }
        }
       }
/* ---------------begining of step down --------------*/
      if(DOWN==1)
      {
       if(delt0[ii]>=tc && delt0[ii]<=t_cell)
       {
        if(t<=delt0[ii])
        {
     ERR_t1[ii]=ERR_t1[ii]+fabs((double)(Qd0-qq2*(1.0-MCR)));
         ERR_t2[ii]=ERR_t2[ii]+qq2*MCR;
        }
        if(t> delt0[ii] && t<=t_cell)
        {
         ERR_t1[ii]=ERR_t1[ii]+fabs((double)(Qd0-qq2));
        }
        if(t>t_cell)
```

```
    {
     if(delt[ii]<=tc)
     {
      if(t<= (t_cell+delt[ii]) )
      {
       ERR_t1[ii]=ERR_t1[ii]+fabs((double)(Qd0-qq1));
      }
      if(t>(t_cell+delt[ii]) )
      {
 ERR_t1[ii]=ERR_t1[ii]+fabs((double)(Qd0-qq1*(1.0-MCR)));
       ERR_t2[ii]=ERR_t2[ii]+qq1*MCR;
      }
     }
     if(delt[ii]>tc)
     {
      ERR_t1[ii]=ERR_t1[ii]+fabs(qq1-Qd0);
     }
    }
   }
   if( delt0[ii]>t_cell)
   {
    if(t<=t_cell)
    {
     ERR_t2[ii]=ERR_t2[ii]+qq2*MCR;
 ERR_t1[ii]=ERR_t1[ii]+fabs((double)(Qd0-qq2*(1.0-MCR)));
    }
    if(t_cell< t && t<=delt0[ii] )
    {
     ERR_t2[ii]=ERR_t2[ii]+qq1*MCR;
 ERR_t1[ii]=ERR_t1[ii]+fabs((double)(Qd0-qq1*(1.0-MCR)));
    }
    if((t_cell+tc)>=t && t>delt0[ii])
    {
     ERR_t1[ii]=ERR_t1[ii]+fabs((double)(qq1-Qd0));
    }
   }
/* STEP DOWN---case delt[ii]< tc  */
   if(delt0[ii] < tc)
   {
    if( t<=t_cell)
    {
      ERR_t1[ii]=ERR_t1[ii]+fabs((double)(Qd0-qq2));
    }
    if( t>t_cell &&  t<= (t_cell+delt[ii]) )
    {
     ERR_t1[ii]=ERR_t1[ii]+fabs((double)(Qd0-qq1));
    }
    if( t> (t_cell+delt[ii]) )
    {
     ERR_t2[ii]=ERR_t2[ii]+qq1*MCR;
ERR_t1[ii]=ERR_t1[ii]+fabs((double)(Qd0-qq1*(1.0-MCR)));
    }
```

```
        }
       }
      }
      t=t+0.1;
    }while(t<(t_cell+tc));
    ERR=0;
    for (ii=EVEN;ii<(N+1);ii++)
    {
       ERR=ERR+2.0*(ERR_t1[ii]+ERR_t2[ii]);
    }
    ERR=F2G*0.1*(ERR-ERR_t1[0]-ERR_t2[0]);
    return ERR;
}
```

```
/* Function for calculating flow distribution and flow
transportation delay for each nozzle */

void flow()
{
   int flag, i, j;
   float dp[15],qo;
   float temp,temp1 ,mu=2.05e-5, Rn;
   float K0, K1, f, den=1.936, pi=3.14159, PL, PU;
   NEGATIVE=0;
   qo=Q/Kscal;
   Qd=qo/NZ;   /* in ft^3/sec */
   Qd0=Q0/NZ/Kscal;
   K1=8.0*K1*den/d/d/d/d/pi/pi/144.0;
   if(EVEN)
   {
      q[0]=qo/2.0;   /* in ft^3/sec   */
      vel[0]=4.0*q[0]/d/d/pi;
      th=lh/(4.0*qo/dh/dh/pi);
      qn[1]=q[0]/N;
      p[1]=qn[1]*qn[1]/Cd/Cd*.9;  /* in psi */
      PL=0.0*p[1]; PU=1.8*p[1];
   }
   if(!EVEN)
   {
      p[0]=1.1*Qd*Qd/Cd/Cd;
      PL=0.0*p[0]; PU=1.8*p[0];
   }
   j=0;
   do
   {
      j=j+1;
      for(i=EVEN;i<(N+1);i++)
      {
         flag=0;
         if(i==0)
         {
            qn[0]=Cd*sqrt(p[0]);
            q[0]=(qo-qn[0])/2.0;
            vel[0]=4.0*q[0]/d/d/pi;
            th=lh/(4.0*qo/dh/dh/pi);
            delt[0]=th;
            pa[0]=p[0]-0.5*den*vel[0]*vel[0]/144.0;
            Rn=vel[0]*d*den/mu;
            f=0.01;
            if(Rn > 2000)
            {
               f=0.001375+0.1375*pow(Rn,-1.0/3.0);
            }
            if(2000>=Rn && Rn!=0.0)
            {
                f=16.0/Rn;
```

```
            }
            dp[i]=0.5/144*f*x*den*vel[i]*vel[i]/d;
            p[i+1]=pa[i]-dp[i];
         }
         if(i!=0)
         {
            temp1=(Cd*Cd*Cd*Cd*K1*K1*q[i-1]*q[i-1]
                  +Cd*Cd*p[i]*(1+Cd*Cd*K1));
            if(temp1<0.0 || p[i]<0.0)
            {
               NEGATIVE=1;
               i=N+1;
               j=1001;
               temp1=0.0;
            }
            if(j!=1001)
            {
               temp=sqrt(temp1);
               qn[i]=(Cd*Cd*K1*q[i-1]+temp)/(1+Cd*Cd*K1);
               q[i]=q[i-1]-qn[i];
               vel[i]=4.0*q[i]/d/d/pi;
               pa[i]=p[i]+K1*den*(vel[i-1]*vel[i-1]
                     -vel[i]*vel[i])/144.0;
               Rn=vel[i]*d*den/mu;
               f=0.01;
               if(Rn > 2000)
               {
                  f=0.001375+0.1375*pow(Rn,-1.0/3.0);
               }
               if(2000>=Rn && Rn!=0.0)
               {
                  f=16.0/Rn;
               }
               dp[i]=0.5/144.0*f*x*den*vel[i]*vel[i]/d;
               p[i+1]=pa[i]-dp[i];
            }
         }
      }
      if( q[N] >= 0.0001*qo)
      {
         PL=p[EVEN];
         p[EVEN]=0.5*(PL+PU);
         flag=1;
      }
      if( q[N] <= - 0.0001*qo)
      {
         PU=p[EVEN];
         p[EVEN]=0.5*(PL+PU);
         flag=1;
      }
   }while (flag==1 && j<100);
   if(j<100)
```

```
    {
        if(EVEN)
        {
            delt[1]=x/2.0/vel[0]+th;
        }
        if(!EVEN)
        {
            pz[0]=p[0];
            delt[1]=x/vel[0]+delt[0];
        }
        for(i=1;i<N;i++)
        {
            pz[i]=0.5*(p[i]+pa[i]);
            delt[i+1]=delt[i]+x/vel[i];
         }
         pz[N]=0.5*(p[N]+pa[N]);
    }
    if(j>=100)NEGATIVE=1;
}
```

REFERENCES

Ahmad SI, Bode LE and Butler BJ (1981) A variable-rate pesticide spraying system. Transactions ASAE 24 (3): 584-589

Anon. (1989) Organic matter on the go. Farm Journal. Mid-March, 18

Anson JH (1983) Technological trends in agricultural electronics. Proceedings of First International Conference on Robotics and Intelligent Machines in Agriculture, Tampa

Bae YH (1987) Mapping yield with a combine instrumented for location detection. Unpublished Ph.D. Dissertation. Texas A&M University Agriculture Engineering

Bajura RA and Jones EH (1976) Flow distribution manifolds. Journal of Fluids Engineering, Transactions ASME 98: 654-666

Bobbe T (1992) Real-time differential GPS for aerial surveying and remote sensing. GPS World 3: 18-22

Bralts VF and Segerlind LJ (1985) Finite element analysis of drip irrigation submain units. Transactions ASAE 28 (3): 809-814

Bryson AE and Ho YC (1981) Applied optimal control. Halsted Press: Washington, D.C.

Buchholz DD and Wollenhaupt NC (1989) Managing field soil fertility variation. Proceedings of 19th North Central Extension-Industry Soil Fertility Conference. St. Louis, 8-9 November, 40-44

Burrough PA (1991) Soil information systems. In: Maguire DJ, Goodchild MF and Rhind DW, Geographic information systems, Volume 2. John Wiley & Sons: New York

Collins EG and Skelton RE (1987) A theory of state covariance assignment for discrete systems. IEEE Transactions on Automatic Control AC-32 (1): 35-41

Compressed Air (1988) The pied piper is changing his tune. Compressed Air Magazine 93 (11): 24-29

Dale RF (1991) Land information systems. In: Maguire DJ, Goodchild MF and Rhind DW, Geographic information systems, Volume 2. John Wiley & Sons: New York

Elliot C (1987) Fertilizer-blending and spreading on-the-go using computerized soil maps and radar guidance. SAE paper 871676

Environmental Systems Research Institute (1991) Understanding GIS. ESRI: Redland, CA

Food and Agriculture Organization of the United Nations (1983) FAO fertilizer handbook, Volume 32. FAO: Rome

Franklin GF, Powell JD and Workman ML (1989) Digital control of dynamic system. Addison-Wesley Publishing Company: Reading, Mass.

Frost AF (1990) A pesticide injection metering system for use on agricultural spraying machines. Journal of Agricultural Engineering Research 46: 55-70

Goering CE (1992) How much and where: economic and environmental concerns increase interest in site-specific crop management; technical advances make it feasible. Agricultural Engineering 73 (4): 13-15

Han S, Goering CE, Hummel JW and Cahn MD (1992) Selection of cell size for site-specific crop management. ASAE paper 927007

Hummel JW (1985) Monitoring and control of field machines. Illinois Research 27 (4): 8-10

Johnston CA (1989) Ecological research applications of geographic information systems. GIS/LIS '89 Proceedings, Volume 2. Orlando, 26-30 November, 569-577

Kepple DD (1987) Unlocking mysteries of cotton yield variation. Agrichemical Age. October, 24A-24B

Koo YM, Young SC and Kuhlman DK (1987) Flow characteristics of injected concentrates in spray booms. ASAE paper 871602

Kruse D (1989) Regional land use tracking in a multi-participant venture. GIS/LIS '89 Proceedings, Volume 1. Orlando, 26-30 November, 187-194

Ksiazek TF (1985) Automatic controls for chemical application. Proceedings of AgriMation 1. Chicago, 25-26 February, 165-172

Kwakernaak H and Sivan R (1972) Linear optimal control systems. Wiley-Interscience: New York

Maciejowski JM (1989) Multivariable feedback design. Addison-Wesley Publishing Company: Reading, Mass.

Massey BS (1985) Mechanics of fluids. Prentice-Hall: London

Merritt HE (1967) Hydraulic control systems. John Wiley & Son: New York

Miller B, Fiez T and Pan W (1992) Impact of landscape variability on grain yield and quality. Proceedings of Precision Farming Variable Cropland for Profit and Conservation. Pullman, Washington, 18 February, 3-6

Miller DS (1971) Internal flow: a guide to losses in pipe and duct systems. British Hydromechanics Research Association Report: Cranfield, Bedford, England

Miller MS and Smith DB (1988) A direct nozzle injection controlled rate spray boom. SAE paper 891611

Motz DS, Searcy SW and Paul EN (1993) PC-MAP: a tool for site specific crop management. SAE paper 933556

Mulla DJ and Hammond MW (1988) Mapping of soil testing results from large irrigation circles. Proceedings of 39th Annual Far West Regional Fertilizer Conference. Bozeman, Montana, 169-176

Ogata K (1970) Modern control engineering. Prentice-Hall: Englewood Cliffs, N.J.

Patel MF (1990) Dynamic modelling of a dual-component controllable fluid fertilizer applicator. Unpublished M.S. Thesis, University of Florida

Paul J (1988) Here come the spud-niks. Agrichemical Age. February, 16A, 16D, 24D

Perold RP (1977) Design of irrigation pipe laterals with multiple outlets. Journal of the Irrigation and Drainage Division, ASCE 103 (IR2): 179-195

Petersen C (1991) Precision GPS navigation for improving agricultural productivity. GPS World 1: 38-43

Peterson CL, He B and Whitcraft JC (1992) Current equipment options for managing variable cropland. Proceedings of Precision Farming Variable Cropland for Profit and Conservation, Pullman, Washington, 18 February, 99-112

Pigford RL, Ashraf M and Miron YD (1983) Flow distribution in piping manifolds. Industrial and Engineering Chemistry Fundamentals 22: 463-471

Sage AP and White CC (1977) Optimum systems control. Prentice-Hall: New York

Safonov MG and Athans M (1977) Gain and phase margin for multiloop LQG regulators. IEEE Transactions on Automatic Control AC-22 (2): 173-179

Schueller JK (1988) Machinery and systems for spatially-variable crop production. SAE paper 881608

Schueller JK (1992) A review and integrating analysis of spatially-variable control of crop production. Fertilizer Research 33: 1-34

Schueller JK and Kulkarni RS (1988) Spatially-variable fluid fertilizer mobile applicator design concepts. SAE paper 881290

Schueller JK and Wang MW (1992) Spatially-variable control of field machinery integrated control theory and a GIS. International Conference on Agriculture Engineering, Paper No. 920607, Uppsala, Sweden, 1-4 June

Shih SF (1989) Geographical information system and GOES image enhancement in rainfall estimation. GIS/LIS '89 Proceedings, Volume 2, Orlando, 26-30 November, 468-477

Stafford JV and Miller PCH (1992) Spatially selective application of herbicide. International Conference on Agriculture Engineering, Paper No. 920620, Uppsala, Sweden, 1-4 June

Taylor RW and McDonald DL (1989) GIS techniques applied to spatial analysis of crime in the city of Dallas, Texas: preliminary findings. GIS/LIS '89 Proceedings, Volume 1, Orlando, 26-30 November, 171-180

Wang MW (1991) Dynamic model of a multi-pump sprayer applicator. Unpublished M.S. Thesis. University of Florida

Whalley D and Schoolmaster FA (1989) A GIS approach to monitoring the impacts of large-scale public developments: the case of D/FW airport. GIS/LIS '89 Proceedings, Volume 1, Orlando, 26-30 November, 314-322

White M (1991) Car navigation systems. In: Maguire DJ, Goodchild MF and Rhind DW, Geographic information systems, Volume 2. John Wiley & Sons: New York

Wilson BJ and Scott JL (1982) Population trends of avena fatua and alopecurus myosuroides on a commercial arable and dairy Farm. Proceedings 1982 British Crop Protection Conference - Weeds, Brighton, 619-628

Wolf B, Fleming J and Batchelor J (1985) Fluid fertilizer manual, Volume 2. National Fertilizer Solutions Association: Peoria, Illinois

Wu I and Gitlin HM (1974) Drip irrigation design based on uniformity. Transactions ASAE 17 (3): 429-432

BIOGRAPHICAL SKETCH

Min-Wen Wang was born in Taiwan, R.O.C., on September 2, 1961. He earned a Bachelor of Science degree in mechanical engineering from Chung-Yuan Christian University in Chungli, Taiwan, in 1984. After graduating from college, he entered the Chung Shan Institute of Science and Technology (CSIST) as a technical officer for military service. He was appointed as a research assistant and worked in the Rocketry Department for four years. He also worked as an assistant engineer at Northman Co., Inc., for three months prior to coming to the United States. At Northman, he studied and practiced hydraulic element design. In 1989, he jointed the Department of Mechanical Engineering of the University of Florida and worked with Dr. Schueller. He received the Master of Science degree in May, 1991.

I certify that I have read this study and that in my opinion it conforms to acceptable standards of scholarly presentation and is fully adequate, in scope and quality, as a dissertation for the degree of Doctor of Philosophy.

John K. Schueller, Chairman
Associate Professor of
Mechanical Engineering

I certify that I have read this study and that in my opinion it conforms to acceptable standards of scholarly presentation and is fully adequate, in scope and quality, as a dissertation for the degree of Doctor of Philosophy.

Jiri Tlusty
Graduate Research Professor
of Mechanical Engineering

I certify that I have read this study and that in my opinion it conforms to acceptable standards of scholarly presentation and is fully adequate, in scope and quality, as a dissertation for the degree of Doctor of Philosophy.

Jacob Hammer
Professor of Electrical
Engineering

I certify that I have read this study and that in my opinion it conforms to acceptable standards of scholarly presentation and is fully adequate, in scope and quality, as a dissertation for the degree of Doctor of Philosophy.

Scot E. Smith
Associate Professor of Civil
Engineering

I certify that I have read this study and that in my opinion it conforms to acceptable standards of scholarly presentation and is fully adequate, in scope and quality, as a dissertation for the degree of Doctor of Philosophy.

Sencer Yeralan
Associate Professor of
Industrial and Systems
Engineering

This dissertation was submitted to the Graduate Faculty of the College of Engineering and to the Graduate School and was accepted as partial fulfillment of the requirements for the degree of Doctor of Philosophy.

August 1994

Winfred M. Phillips
Dean, College of Engineering

Karen A. Holbrook
Dean, Graduate School